

The Birth Environment of the Solar System

Fred C. Adams

Michigan Center for Theoretical Physics

Physics Department, University of Michigan, Ann Arbor, MI 48109, USA

to appear in Annual Reviews of Astronomy and Astrophysics (2010, Volume 48)

ABSTRACT

This paper reviews our current understanding of the possible birth environments of our Solar System. Since most stars form within groups and clusters, the question becomes one of determining the nature of the birth aggregate of the Sun. This discussion starts by reviewing Solar System properties that provide constraints on our environmental history. We then outline the range of star-forming environments that are available in the Galaxy, and discuss how they affect star and planet formation. The nature of the solar birth cluster is constrained by many physical considerations, including radiation fields provided by the background environment, dynamical scattering interactions, and by the necessity of producing the short-lived radioactive nuclear species inferred from meteoritic measurements. Working scenarios for the solar birth aggregate can be constructed, as discussed herein, although significant uncertainties remain.

Subject headings: Cluster Dynamics, Nuclear Abundances, Planet Formation, Star Formation, Stellar Clusters, Supernovae, and the Sun

1. INTRODUCTION

Some of the most foundational questions in astrophysics are those of “origins”, including the formation of the universe, galaxies, stars, and planets. On each of these fundamental scales, astronomical entities are brought into existence through complex physical processes, live out their lives, and often end with death-like finality. The origin of the universe and galaxy formation fall in the domain of cosmology, although these scales are largely decoupled from the question of solar birth. On smaller scales, star formation and planet formation are intimately connected, since planets form within the circumstellar disks that arise from protostellar collapse. In this regime, the origin of our own star and its planetary system represents a fundamental astronomical issue.

Recent studies have underscored the finding that most stars are not born in isolation, but rather form within groups and clusters (e.g., Carpenter 2000, Lada & Lada 2003, Porras et al. 2003). Although some fraction of the stellar population does form in an isolated mode (e.g., in the nearby Taurus star-forming region), the considerations of this review suggest that our Solar System formed within a group or cluster with some membership size N . This state of affairs thus poses a number of coupled questions considered herein: What was the size N of the solar birth cluster? What constraints can we place on the properties of the solar birth aggregate? How did the solar birth environment influence the formation of our planetary system? How rare or common are the necessary conditions that gave rise to our Solar System?

At the current epoch, the Solar System is nearly five billion years old (more precisely, about 4600 Myr). As outlined above, stars form in groups and clusters that are embedded within molecular clouds, and these clouds have lifetimes measured in only tens of millions of years (or even less — see Hartmann et al. 2001). Within the clouds, the clusters themselves also live for tens of millions of years, or somewhat shorter times. Even the long-lived open clusters dynamically evaporate over hundreds of millions of years. As a result, the birth environment of the Sun has long since been dissipated. Nonetheless, as reviewed herein, the extant properties of our Solar System, coupled with our emerging understanding of star and planet formation processes, allow us to reconstruct some of the requirements of the birthplace of the Sun.

One reason for constraining the solar birth environment is because of its intrinsic interest. In addition to the issue of where we came from, however, the origin of our Solar System provides an important consistency check on the current paradigms of star and planet formation. These theories have been tested and modified over the past decades, and now provide a compelling picture for the origin of stars and planets. However, the properties of our Solar System are known in much greater detail than those in other systems. As a result, our Solar System represents an important additional test of the theoretical framework. In particular, we would like our theories of star/planet formation to produce solar systems with roughly the properties of our own under unremarkable circumstances, i.e., under conditions that are relatively common in observed star forming regions.

1.1. Scope of this Review

This review focuses on three general types of physical process that influence solar system formation and thereby constrain the possible birth environment of the Sun:

[1] The birth cluster affects star and planet formation through dynamical processes, including disk truncation and perturbations of planetary orbits due to passing stars. The observed lack of severe disruption provides an upper limit on the density of the birth cluster and the time that the Solar System lived in such an environment. On the other hand, the observed orbital elements of Sedna (and perhaps other Kuiper Belt objects) can be explained by such close encounters, so that some type of dynamical interactions may be required.

[2] The birth cluster also provides strong background radiation fields, including those at ultraviolet (UV) wavelengths. These fields can drive the evaporation of the early solar nebula and hence the loss of planet forming potential. Gas removal from the outer nebula also affects the edge structure of the Solar System. Harder radiation (X-rays and EUV photons) provides ionization, which can influence both the early star formation process and the subsequent evolution of our circumstellar disk.

[3] The presence of short-lived radioactive species inferred from meteorites provides another class of constraints. Radioactive nuclei can be produced in supernova explosions, evolved stars, and by internal irradiation mechanisms. Under the assumption that some external enrichment is necessary, we obtain further constraints. In particular, the cluster must be relatively large, the Sun must reside within a confined range of radial locations, and the proper timing of events must be realized.

This review considers these three classes of constraints, and includes a general assessment of how star forming clusters can potentially affect their constituent solar systems. In this respect, this review differs from many previous discussions that primarily focus on the origin of the short-lived radio isotopes (Wadhwa et al. 2007; Goswami & Vanhala 2000; Busso et al. 1999, 2003; Wasserburg et al. 2006) and/or the thermodynamic history of the early solar system (e.g., Krot et al. 2005ab, 2008). Although these issues are discussed herein, the reader is referred to these earlier reviews for additional details regarding radio isotopes and heating in the early solar nebula (see also Montmerle et al. 2006).

This discussion of the solar birth aggregate involves two coupled themes: First, significant tension exists between the apparent need for a large birth cluster to provide nuclear enrichment and to explain Sedna’s orbit, and the need for a smaller, less interactive cluster to avoid overly disruptive dynamical and radiative effects. The required compromise underscores the need for quantitative assessments of the physical processes that inform the properties of the solar birth environment. Second, as outlined below, many of these constraints must be addressed statistically. For example, clusters do not fully sample the high end of the stellar IMF, so that supernova enrichment does not occur with certainty, but rather with a well-defined probability distribution. Similarly, clusters are highly chaotic systems, so that dynamical issues must also be addressed in terms of probabilities.

1.2. Overview

This paper is organized as follows. In Section 2, we outline some of the basic characteristics of our Solar System, with a focus on those properties that provide clues to the past. The range of possible birth environments is discussed in Section 3, along with an overview of cluster properties. The constraints on these clusters provided by dynamical considerations are discussed in Section 4. The radiation fields produced by various star forming environments are then considered in Section 5, along with an overview of their possible effects on young and forming stars. These results are then combined with Solar System properties to obtain further constraints on the birth environment. The question of short-lived radioactive isotopes, as inferred from meteoritic data, is taken up in Section 6. This discussion includes the two leading explanations for these radionuclides, internal irradiation mechanisms and external enrichment through supernovae. The review concludes in Section 7 with an overview of the constraints, possible scenarios for the solar birth aggregate, and a discussion of the general implications for star/planet formation.

2. SOLAR SYSTEM PROPERTIES

2.1. The Sun and the IMF

The Sun is a relatively large star. Of the 50 nearest stars, the Sun ranks a respectable fourth largest in terms of mass (e.g., see Henry et al. 1994 and subsequent papers). In contrast, the distribution of stellar masses at the epoch of formation, the stellar IMF, is heavily weighted toward stars of low mass (e.g., Scalo 1998). A useful way to parameterize the stellar IMF is to define \mathcal{F}_1 to be the fraction of the stellar population with masses greater than the Sun. Observations indicate that $\mathcal{F}_1 \approx 0.12$. In other words, the fact that our Sun is a relatively large star is a ~ 12 percent effect. As a result, the mass of the Sun is somewhat large but still unremarkable.

In considering the possible range of birth environments, we need to consider effects from the full distribution of stellar masses, especially the high mass end. The largest stars provide the largest potential impacts on star and planet formation, where these effects include radiation, winds, and supernova explosions. The mass distribution for massive stars can be written in power-law form,

$$\frac{dN_*}{dm} = \mathcal{F}_1 \gamma m^{-(\gamma+1)}, \quad (1)$$

where m is the mass in Solar units and the index $\gamma \sim 1.35$ (Salpeter 1955). Although the low-mass end of the IMF has received considerable attention in recent years, the power-law

form for the high-mass end remains robust. However, the value of the index γ appears to have considerable scatter from region to region (Scalo 1998), such that γ is evenly distributed within the range $\gamma = 1.5 \pm 0.5$. For the sake of definiteness, in this review we use $\gamma = 1.5$ to characterize the high-mass end of the IMF, but the reader should note that a range of values is allowed.

Note that the probability distribution of equation (1) is normalized so that

$$\int_1^\infty \frac{dN_*}{dm} dm = \mathcal{F}_1. \quad (2)$$

Since the IMF has an upper mass limit at $m \equiv m_\infty \approx 100$, the above integral introduces a correction factor $[1 - (1/m_\infty)^\gamma] \approx 0.998$ in the normalization; we neglect this correction in the present discussion.

2.2. The Sun as a Single Star

The Sun is a single star, whereas the majority of solar-type stars are found in binary systems (Abt 1983, Duquennoy & Mayor 1991). However, about one third of solar-type stars are single, so that the lack of a binary companion in our Solar System does not represent a significant constraint. A single Sun corresponds to a ~ 30 percent effect. For completeness, we also note that since most stars are much smaller than the Sun, and smaller stars are primarily single, the majority of all stars are actually single (Lada 2006). Although the Sun ended up as a single star, it remains possible for the Sun to have had binary companions earlier in its history (see the discussion of Malmberg et al. 2007). Any such companions must have had wide orbits, however, so as not to disrupt the early solar nebula and/or the planetary orbits.

2.3. Solar Metallicity

The Sun has relatively high metallicity (Wielen et al. 1996, Wielen & Wilson 1997). For G dwarfs in the Solar neighborhood, the metallicity distribution has a peak at $[\text{Fe}/\text{H}] = -0.20$ dex (Rocha-Pinto & Maciel 1996). For the same distribution, only about one fourth of the G dwarfs have metallicity as large as the Sun, so that the moderately high metal content of the Solar System corresponds to a 25 percent effect. We also note that some of the metallicity could be contributed by the supernova that is thought to have enriched the solar system in short-lived radioactive species. On a related note, the abundances of oxygen isotopes in the Solar System, in particular the ratio $^{18}\text{O}/^{17}\text{O}$, show interesting anomalies that

could indicate pollution by a nearby supernova (Young et al. 2009). On the other hand, these anomalies could also be explained by isotope selective photodissociation in the early solar nebula (Smith et al. 2009).

2.4. Planets and their Orbits

One important feature of our Solar System is that it has produced a substantial number of planets, including giant gaseous planets in the outer regions and rocky terrestrial planets further inward. Although observations of extra-solar planetary systems indicate that giant planets are not rare, planet formation is not guaranteed. Current data suggest that about 10 percent of solar-type stars harbor giant planets with semi-major axes in the range $a = 0.02 - 5$ AU (Cummings et al. 2008). Since the observational sample is not complete, especially for planets with longer periods, the fraction of solar-type stars with giant planets is even larger. After extrapolating the data to include the full range of periods, the fraction of systems with giant planets is estimated to be about 20 percent (although larger fractions, perhaps up to 50 percent, remain possible).

At this time, detection of planets with masses comparable to Earth is just out of reach for main-sequence stars (due to technical limitations). As a result, it is too early to assess the odds of solar systems having terrestrial planets. However, a number of considerations suggest that such planets can be made relatively easily: We first note that terrestrial mass planets have been detected in orbit about pulsars (Wolszczan 1994). In addition, our Solar System has readily produced not only four terrestrial planets, but a large collection of moons, asteroids, dwarf planets, and comets. Data from extrasolar planets show that the planetary mass function increases toward lower masses. These findings argue that the formation of terrestrial planets should be common (and hence that our Solar System is not rare in this regard).

One of the most remarkable features of our Solar System is that the planetary orbits are well-ordered. More specifically, all of the planetary orbits are nearly in the same plane, with inclination angles in the narrow range $(\Delta i) \leq 3.5^\circ$. Another measure of order is the low orbital eccentricities, which lie in the range $0 \leq e \leq 0.2$. If Mercury is excluded, the next largest eccentricity is that of Mars at $e \approx 0.09$. As discussed below, orbital eccentricities and inclination angles are relatively easy to excite by passing stars and other dynamical perturbations. As a result, the currently observed order of the Solar System provides powerful constraints on its history.

On a related note, observations of extrasolar planets (e.g., Schneider 2009) show that

planetary orbits in other solar systems display a wide range of eccentricities. More specifically, for extrasolar planets with semi-major axes $a \geq 0.1$ AU, the mean of the distribution is approximately $\langle e \rangle \approx 0.3$ and the median is $e_h \approx 0.24$. Orbits with smaller semi-major axes tend to be circularized by tidal interactions with the central star. The inclination angles of extrasolar planetary systems are difficult to measure. Nonetheless, available data indicate that the currently observed multi-planet systems are more dynamically active, and significantly less well-ordered, than our own (e.g., Udry & Santos 2007).

2.5. Edges of the Solar System

The Solar System has a number of outer “edges”, which provide further constraints on its dynamical past. The first obvious edge is marked by the planet Neptune, which orbits with a semi-major axis $a \approx 30$ AU. The solar nebula must have extended out to (approximately) this radius in order to facilitate planet formation.

Beyond the last giant planet, the Solar System contains a large collection of smaller rocky bodies in the Kuiper Belt. The orbits of these Kuiper Belt objects, as a group, have much larger eccentricities and inclination angles than the planetary orbits (Luu & Jewitt 2002). The Kuiper belt is thus dynamically excited, to a moderate degree, and this property must be consistent with scenarios for solar birth. In spite of their large numbers, these bodies contain relatively little total mass, which has been estimated to be 10 – 100 times less than the mass of Earth (Bernstein et al. 2004). The outer boundary of the planetary system (and inner boundary of the Kuiper belt) at 30 AU is thus significant. In addition, although the outer edge of this belt is not perfectly sharp, a significant drop-off is observed around 50 AU (Allen et al. 2000). This radial location roughly corresponds to the 2:1 mean motion resonance with Neptune. Since, in principle, additional bodies could have formed and survived beyond this radius, the origin of this edge at ~ 50 AU represents an important issue.

At still greater distances, the Solar System contains a large, nearly spherical collection of comets known as the Oort Cloud. This structure extends to about 0.3 pc ($\sim 60,000$ AU). Since the comets in the Oort Cloud are loosely bound to the Sun, gravitational perturbations from passing stars can easily disrupt the cloud. From the impulse approximation, the change in velocity of the Sun due to a passing star is approximately given by $\Delta v = 2GM_*/(bv_\infty)$, where b is the distance of closest approach. Setting the orbit speed (at radius b) of the comets equal to this change in velocity, we obtain an estimate for the radius of the sphere

in which the Sun can protect its comets:

$$r \approx \frac{4GM_*^2}{M_\odot v_\infty^2} \approx 0.017 \text{pc} \left(\frac{v_\infty}{1 \text{ km s}^{-1}} \right)^{-2}, \quad (3)$$

where the numerical value assumes both the Sun and the passing star have the same mass. For typical interaction rates, stellar densities, and encounter speeds in embedded clusters, where the Sun might have formed, most of the Oort cloud would be stripped by passing stars. As a result, this structure probably formed later, after the Sun left its birth environment. In addition, the Oort cloud is likely to have grown slowly, over perhaps 1 Gyr (Duncan et al. 1987), i.e., a timescale much longer than the expected lifetime of the birth cluster. Nonetheless, the possible timing of close encounters is constrained by models of Oort cloud formation (Levison et al. 2004, Brasser et al. 2006, Kaib & Quinn 2008).

2.6. Minimum Mass Solar Nebula

Given the basic architecture of the Solar System described above, it is customary to define a benchmark disk model known as the Minimum Mass Solar Nebula (often denoted as MMSN). Since the planets are currently enriched in heavy elements relative to the Sun, one must add back in the mass of the gas required for the augmented system to have solar metallicity. Although this exercise is not without uncertainties, a standard version of the early solar nebula can be defined. This disk has surface density $\Sigma(r)$ and temperature $T(r)$ profiles of the power-law form

$$\Sigma(r) = \Sigma_1 \left(\frac{1 \text{ AU}}{r} \right)^p \quad \text{and} \quad T(r) = T_1 \left(\frac{1 \text{ AU}}{r} \right)^q, \quad (4)$$

where Σ_1 and T_1 are the values at $r = 1 \text{ AU}$, and where $p \approx 3/2$ and $q \approx 1/2$. The surface density at 1 AU is estimated to lie in the range $\Sigma_1 \approx 2000 - 4500 \text{ g cm}^{-2}$ (e.g., Weidenschilling 1977, Hayashi 1981). Using the upper end of this range and assuming that the nebula extends out to $r_d = 30 \text{ AU}$, the enclosed mass is estimated to be $M_d \approx 0.035 M_\odot$. Keep in mind that this model is only a reference point; for example, recent observations suggest that $p \approx 1$ with lower disk masses (Andrews et al. 2009), whereas disk accretion rates argue for higher starting masses $M_d \approx 0.1 M_\odot$ (Hartmann 2007). Since planets can migrate, the starting surface density of the nebula is subject to further uncertainty (compare Desch 2007 and Crida 2009).

2.7. Short-lived Radioactive Isotopes

One of the most intriguing — and potentially constraining — properties of our Solar System is the inferred presence of short-lived radioactive species during the epoch of planet formation. For the sake of definiteness, we consider “short-lived” species to be those with half-lives less than about 10 Myr. The presence of these radio isotopes is inferred by measuring the daughter products in meteoritic samples, which condensed into rocks during the formative stages of the Solar System. These short-lived radioactive species thus indicate that only a short time (perhaps ~ 1 Myr) could have elapsed between their production and their subsequent incorporation into early Solar System material. A viable source of these short-lived radio isotopes is thus indicated (for recent reviews, see Wasserburg et al. 2006, Wadhwa et al. 2007, and references therein).

Table I lists some of the most important radio isotopes, including ^{10}Be , ^{26}Al , ^{41}Ca , ^{60}Fe , ^{53}Mn , ^{107}Pd , and ^{182}Hf . The half-lives, daughter products, reference isotopes, and fractional abundances are also given (see Wasserburg 1985, Cameron 1993, Goswami & Vanhala 2000, McKeegan et al. 2000, and many others). Additional measurements indicate the presence of radionuclides with somewhat longer lifetimes, e.g., ^{129}I , and ^{244}Pu , with half-lives of about 16 Myr and 80 Myr, respectively. Here we assume that these longer-lived species can be explained by galactic-scale nucleosynthesis coupled with mixing in the interstellar medium, so that they do not constrain the birth environment (see Wasserburg et al. 2006). In contrast, the short-lived species must be produced locally, near the time and location of solar birth, i.e., on time scales measured in Myr and distances measured in pc (see below). These short-lived nuclei thus provide potential constraints on the birth cluster.

Table I: Radio Isotopes

Nuclear Species	Daughter	Reference	Half-life (Myr)	Mass Fraction
^7Be	^7Li	^9Be	53 days	(8×10^{-13})
^{10}Be	^{10}B	^9Be	1.5	$(\sim 10^{-13})$
^{26}Al	^{26}Mg	^{27}Al	0.72	3.8×10^{-9}
^{36}Cl	^{36}Ar	^{35}Cl	0.30	8.8×10^{-10}
^{41}Ca	^{41}K	^{40}Ca	0.10	1.1×10^{-12}
^{53}Mn	^{53}Cr	^{55}Mn	3.7	4.0×10^{-10}
^{60}Fe	^{60}Ni	^{56}Fe	1.5	1.1×10^{-9}
^{107}Pd	^{107}Ag	^{108}Pd	6.5	9.0×10^{-14}
^{182}Hf	^{182}W	^{180}Hf	8.9	1.0×10^{-13}

3. DEMOGRAPHICS OF STAR-FORMING REGIONS

3.1. Distribution of Clusters

Given that most stars form within stellar groups and clusters, it is useful to assess the possible range of these birth environments. Unfortunately, at this time, the field has not reached a consensus regarding the distribution of group/cluster sizes. The membership of these aggregates varies from $N = 1$ (corresponding to stars forming in isolation) up to about $N \approx 10^6$ (corresponding to proto-globular clusters). The relative frequency of these environments is determined by the distribution df_c/dN , which is defined here to be the probability that a cluster has membership size N . The corresponding probability that a given star (or solar system) finds itself born within a system of membership size N is then given by

$$\frac{dP}{dN} = N \frac{df_c}{dN}, \quad (5)$$

with a normalization such that

$$\int_1^\infty \frac{dP}{dN} dN = 1. \quad (6)$$

For surveys in the solar neighborhood, where clusters are found with membership size in the range $N = 100 - 2000$, the distribution of cluster number $df_c/dN \propto 1/N^2$, so that the probability density for a star being born in a system of size N has the form $dP/dN \propto 1/N$ (e.g., see Carpenter 2000, Kroupa & Boily 2002, Lada & Lada 2003, Porras et al. 2003). The integral of this distribution indicates that the cumulative probability $P \sim \ln N$, so that the probability of stars being born in birth aggregates of varying size N is evenly logarithmically distributed across the range in N .

A similar result is found for larger clusters, where the observational samples are farther away and less complete (especially at the lower end of the distribution). In this regime, observations suggest that the distribution also has the form $df_c/dN \propto N^{-2}$ for values of N up to and including those of globular clusters (Elmegreen & Efremov 1997). Given that both the solar neighborhood and the realm of large clusters (roughly $N \geq 2000$) have distributions of the form $df_c/dN \sim N^{-2}$, the simplest hypothesis is to assume that the same law holds over the entire range of N . In this case, stars would form with equal probability in each decade of N . This hypothesis is equivalent to assuming that the normalizations of the distributions match up. For purposes of estimating the probability of the Solar System being born in clusters of various sizes, we will use this simple, log-random distribution. However, the reader should keep in mind that not enough data exist for this hypothesis to be verified.

Two additional issues introduce further uncertainty in defining the distribution of cluster sizes:

[1] Although many discussions dismiss the importance of isolated star formation, sometimes called the distributed population, results from the *Spitzer* Space Telescope (which provides an unbiased survey) indicate otherwise: Let N_M be the “median point” of the distribution, so that half of the stars form within clusters of size $N < N_M$ and the other half form within clusters $N > N_M$. For the solar neighborhood surveys (Lada & Lada 2003, Porras et al. 2003), this median point has the value $N_M \approx 300$ (Adams et al. 2006). When the distributed population is included, however, the median point of the probability distribution moves downward to $N_M \approx 100$ (Allen et al. 2007).

[2] It is generally accepted that only about 10 percent of the stellar population is born within systems that are destined to become open clusters, which are gravitationally bound over longer timescales of 100 – 500 Myr (e.g., van den Bergh 1981, Elmegreen & Clemmens 1985, Battinelli & Capuzzo-Dolcetta 1991, Adams & Myers 2001). Suppose that the probability distribution for star-forming units has equal weight for each decade in N , as would be the case if the distribution in the solar neighborhood extends upward as described above. In this case, half of the stellar population would be born within systems with $N \geq 1000$, but at most 20 percent of that population would end up living in open clusters. In this case, the remaining 80 percent of the stars would be born within “clusters” that dissolve quickly, after only ~ 10 Myr, a timescale that is shorter than the relaxation time for these systems. As outlined below, this timescale is also shorter than that required to explain many Solar System properties. As a result, some evidence points toward the Sun being born within a gravitationally bound cluster, as opposed to a short-lived aggregate, and this requirement is realized for only about 10 percent of the stellar population.

In light of these uncertainties, the distribution df_c/dN of cluster membership sizes should be considered preliminary. More data are required to clear up these uncertainties.

3.2. Cluster Properties

In addition to the issue of what cluster size distribution df_c/dN (dP/dN) applies, several other issues arise. In particular, the stellar membership size N is not the only relevant variable. Clusters with the same N can have varying radii and hence varying mean densities. On a finer scale of distinction, clusters with the same size N and radius R can have different distribution functions for the stellar velocities, different stellar density profiles, or different background potentials given by their gaseous component. In the past several years, observations have started to place constraints on the possible ranges of the cluster parameters, especially for the clusters in the solar neighborhood (those within ~ 2 kpc of the Sun). A brief overview of these properties can be summarized as follows (see Allen et al. 2007;

Gutermuth et al. 2005, 2009; Lada & Lada 2003; Porras et al. 2003; and references therein):

The mean cluster radius R scales with cluster membership size N according to the power-law relation

$$R = R_0 \left(\frac{N}{N_0} \right)^\alpha . \quad (7)$$

For clusters in the solar neighborhood (Lada & Lada 2003, Porras et al. 2003), this law holds with parameters $R_0 = 1$ pc, $N_0 = 300$, and $\alpha \approx 1/2$ (Adams et al. 2006). This relationship defines the mean radius for a given N ; the data show a scatter on either side of this mean value with an amplitude of approximately a factor of 2. For the full range of clusters, extending up to $N = 10^6$, equation (7) predicts overly large radii for large- N clusters if we use index $\alpha = 1/2$ (compare with data presented in Chandar et al. 1999, Pfalzner 2009; see also Proszkow 2009). Over this full range of cluster membership sizes, indices in the range $\alpha \approx 1/4 - 1/3$ provide a better fit.

With the cluster radii specified through equation (7), the characteristic mean stellar density $\langle n_* \rangle$ is given by

$$\langle n_* \rangle = \frac{3N}{4\pi R^3} \propto N^{1-3\alpha} . \quad (8)$$

For $\alpha = 1/2$ ($1/4$), the stellar density decreases (increases) with membership size N . In either case, however, the mean stellar density is a relatively slowly varying function of N . Note that the intermediate value $\alpha = 1/3$ leads to a constant stellar density. Further, the typical mean value of the stellar density is of order $\langle n_* \rangle \sim 100$ pc $^{-3}$. This density affects the interaction rates, and hence the probability that the early Solar System suffered a close encounter with a passing star (see below).

Observations of cluster-forming molecular cloud cores show that the gas density profiles have the approximate form $\rho \sim 1/r$ so that the enclosed mass $M(r) \sim r^2$ (Larson 1985, Jijina et al. 1999). Similarly, N-body simulations of young embedded clusters show that the stellar number density also has a power-law form $n_* \sim 1/r^p$, with index p close to unity (e.g., Kroupa 1995). For purposes of this discussion, we need to estimate the probability that the Solar System resides at a given radial location within a cluster. We can thus use the probability distribution

$$\frac{dP}{dr} = \frac{4\pi r^2}{N} n_*(r) = \frac{2r}{R^2} , \quad (9)$$

where R is the cluster radius and where the distribution is normalized so that $\int_0^R (dP/dr) dr = 1$. The probability distribution dP/dr thus vanishes outside the cluster where $r > R$. The corresponding expectation value for the radial position is given by $\langle r \rangle = 2R/3$, and the median radius is given by $r_h = \sqrt{2}R/2$. This form is valid for young clusters. At later times,

the density profile is expected to become steeper and approach the form $n_* \sim r^{-2}$, so that $dP/dr \approx 1/R$; for this case, $\langle r \rangle = R/2 = r_h$.

3.3. Cluster Dynamics

The relaxation time t_R defines the clock that sets the pace for cluster dynamics (Binney & Tremaine 1987). For embedded clusters that contain a substantial gaseous component, the relaxation time is given approximately by

$$t_R \approx \frac{v}{R} \frac{N}{10\epsilon^2 \ln(N/\epsilon)}, \quad (10)$$

where v/R is the crossing time, N is the cluster membership size, and $\epsilon = N\langle m_* \rangle/M_C$ is the star formation efficiency; here, $\langle m_* \rangle$ is the mean stellar mass and M_C is the total cluster mass, including gas (Adams & Myers 2001). While the cluster retains its gaseous component, the relaxation time is thus longer than that of purely stellar systems (Binney & Tremaine 1987). The behavior of the gas content thus plays an important role in early cluster evolution (the first ~ 5 Myr).

Massive stars sink to the cluster center over a relatively long time scale, given approximately by t_R/m , where t_R is the dynamical relaxation time (e.g., equation [10]) and m is the mass of the star in solar masses (Portegies Zwart 2009). Of course, the massive stars can also be formed at the cluster centers, and some observational evidence (Testi et al. 2000) and theoretical considerations (Bonnell & Davies 1998) support this point of view. On the other hand, mass segregation can be sped up through a combination of subvirial starting velocities and sufficiently clumpy initial density distributions (Allison et al. 2009, Moeckel & Bonnell 2009). In any case, massive stars are expected to reside near cluster centers.

For gravitationally bound systems, where about 10 percent of the stellar population is born, the total lifetime t_T of a cluster is expected to be a multiple Q of the relaxation time t_R (Binney & Tremaine 1987), where $Q = 10 - 100$. If we use the definition of t_R , the virial relation $v^2 = GM/R$, and the number versus radius relation of equation (7), the expected cluster lifetime scales according to $t_T \sim N^{3/4}/\ln N$, where we have used $\alpha = 1/2$. For comparison, the timescale over which observed star clusters are dissolved obeys an empirical law of the form $t_T = 2.3 \text{ Myr } M^{0.6}$, where the cluster mass M is given in solar masses (Lamers et al. 2005). For $M = 300$, this empirical relation implies that $t_T \approx 70 \text{ Myr}$. Since the relaxation time for this type of cluster is $t_R \approx 5 \text{ Myr}$, we get agreement for $Q \approx 14$.

In any case, clusters live for timescales that are much shorter than the current age of the Solar System. It is interesting to determine how many orbits the Solar System has

made around the galactic center since its birth. The circular velocity of the Sun around the Galaxy is $v_{\text{cir}} \approx 235 \text{ km s}^{-1}$. If we assume that the orbit speed and galactocentric radius R_g have not changed, this exercise implies that the solar system has made about $N_{\text{orb}} = (v_{\text{cir}}t)/(2\pi R_g) \approx 22$ orbits. The Solar System has thus traveled an enormous distance (more than one Mpc) since its birth. Note that the Solar System is likely to have experienced many (wide) encounters that change its velocity vector during the course of its lifetime. As outlined in the following section, however, the Solar System is unlikely to have experienced close encounters with any passing stars, as such perturbations would have left dramatic — and unobserved — signatures in our planetary orbits.

4. CONSTRAINTS FROM DYNAMICS

4.1. Encounter Rates in Embedded Clusters

Within a cluster, the rate Γ at which a given solar system encounters other stellar members can be written in the form

$$\Gamma = \langle n\sigma v \rangle, \quad (11)$$

where n is the number density of potential target systems, σ is the cross section for the given interaction, and v is the typical speed at which the solar system orbits through the cluster. The velocity and number density vary with time and with position in the cluster, so that averaging is necessary, as indicated by the angular brackets. In addition, interaction cross sections depend on the encounter speeds.

For a given cluster, we define $\Gamma(b)$ to be the rate at which a given solar system encounters passing stars within a distance b . Numerical (N-body) simulations show that this encounter rate can be written in the form

$$\Gamma = \Gamma_0 \left(\frac{b}{b_0} \right)^\eta, \quad (12)$$

where Γ_0 and η are constants, b is the distance of closest approach, and b_0 is a reference distance scale (Proszkow & Adams 2009). In the absence of gravitational focusing, the index $\eta \approx 2$; in practice, one finds somewhat smaller values in the range $\eta = 1-2$, where η decreases slowly with the range of close encounters under consideration. Without loss of generality, we can take $b_0 = 1000 \text{ AU}$. The constant Γ_0 depends on the specifics of the cluster properties; for the parameters expected for possible solar birth clusters, Γ_0 typically lies in the range $\Gamma_0 = 0.01 - 0.1$ encounters per star per Myr. These values can be understood as follows: For clusters in the present-day solar neighborhood, the mean stellar density is about $n_0 \approx 100 \text{ pc}^{-3}$, and the typical velocity dispersion $v_0 \approx 1 \text{ km s}^{-1}$. The nominal value of $\Gamma_0 \sim n_0 v_0 b_0^2$ is

thus of order $\Gamma_0 \sim 0.0025 \text{ Myr}^{-1}$. The actual value of Γ_0 is larger because the clusters start with subvirial conditions and spend much of their embedded phase with larger densities; the clusters thus contract by a factor of about $\sqrt{2}$ in radial scale and hence a factor of about $2\sqrt{2}$ in density. In addition, the interactions are more frequent in the cluster core, where the density is higher, and this effect also increases Γ_0 .

For a given timescale t_C , the above considerations define a characteristic distance of closest approach, denoted here as b_C . By setting $\Gamma t_C = 1$ in the interaction rate of equation (12), we find the characteristic distance scale b_C for close encounters over that span of time, i.e.,

$$b_C = b_0(\Gamma_0 t_C)^{-1/\eta}. \quad (13)$$

Note that the lifetime of embedded clusters (Allen et al. 2007), the expected lifetime of circumstellar disks (Hernández et al. 2007), and the time required to form giant planets (Lissauer & Stevenson 2007) are of order 3 – 10 Myr. For the sake of definiteness, we set $t_C = 10 \text{ Myr}$ and find that $b_C \approx 300 - 1000 \text{ AU}$. In this sense, the “typically expected” distance of closest approach experienced by the early solar system is several hundred AU (Bonnell et al. 2001, Adams et al. 2006, Malmberg et al. 2007). For other parameter choices, the distance scale b_C can be found using equation (13).

4.2. Orbital Considerations

Another relevant property of clusters is their distribution of orbits. Compare the extreme cases of purely radial orbits and purely circular orbits: For radial orbits, solar systems pass through (or near) the cluster center every crossing time ($\sim 1 \text{ Myr}$). The cluster center is the densest region, and contains the most massive stars, so radial orbits lead to maximal disruption in terms of both radiation exposure and probability of scattering encounters. In contrast, for a given orbital energy, circular orbits allow solar systems to stay as far as possible from the cluster center and thereby minimize the probability of disruption.

One standard way to characterize the orbits in a dynamical system is to define the parameter β according to

$$\beta \equiv 1 - \frac{\langle v_\theta^2 \rangle}{\langle v_r^2 \rangle}, \quad (14)$$

where v_r and v_θ are the radial and poloidal components of the velocity (Binney & Tremaine 1987). Isotropic distributions of velocity lead to $\beta = 0$, whereas radial orbits result in $\beta = 1$.

Observations of young embedded clusters are starting to provide clues to the expected

values of β . Growing observational evidence suggests that forming stars in clusters are not born with virial velocities (Walsh et al. 2004, Peretto et al. 2006). Instead, the clumps that collapse to form stars move more slowly through the system, and only begin to move ballistically after star/disk formation is complete. With these subvirial starting conditions, the initial orbits are directed more radially inward (compared with virial starting states) and some dynamical memory of this initial condition is retained (Adams et al. 2006). The loss of the gaseous component in young clusters can induce an additional radial component to the stellar velocities. As a result, subvirial starting conditions lead to $\beta \approx 1/2$, a value intermediate between radial and circular orbits. On a related front, kinematic observations of stars in young clusters are now possible, and recent data indicate that the Orion Trapezium Cluster displays the kinematic signatures of subvirial starting conditions (Tobin et al. 2009, Proszkow et al. 2009). These observational considerations, while indirect, suggest that forming clusters generally have moderately radial velocity distributions. This finding, in turn, increases the probability of solar system disruption through both radiation exposure and scattering encounters. For the future, it would be useful to have further observational specification of cluster velocity distributions to help assess environmental effects.

4.3. Disk Truncation

During the early stages of solar system formation, close encounters by passing stars can disrupt the solar nebula and thereby limit the mass reservoir available for planet formation (Clarke & Pringle 1993, Ostriker 1994, Heller 1995, Kobayashi & Ida 2001; see also Kenyon & Bromley 2001 for a discussion of the effects of gravitational stirring). Taken together, these studies show that passing stars act to truncate circumstellar disks during close encounters. If b is the impact parameter of the encounter, the disks are generally truncated at a radius $r \approx b/3$. Most of the material outside this truncation radius is either left unbound, or is captured by the passing star. In addition, the surface density of the remaining disk (inside the truncation radius $r = b/3$) is perturbed during the encounter.

As outlined in Section 2.5, the inferred gas surface density of the early solar nebula has a relatively sharp edge at $r \approx 30$ AU. This estimate is based on reconstituting the nebula based on the masses, compositions, and orbits of the planets. Although this procedure is not without uncertainties, the edge at approximately 30 AU remains a robust result. This finding constrains any close encounters that took place while the early solar nebula was intact to have impact parameters $b \geq 90$ AU. Since the timescale for giant planet formation (Lissauer & Stevenson 2007) and the expected lifetimes of circumstellar disks (Hernández et al. 2007) are both about 10 Myr, this constraint applies over the first ~ 10 Myr of Solar

System history.

Using equation (12), we can estimate the rate at which the early Solar System experienced close encounters with $b < 90$ AU: This rate is expected to fall in the range $\Gamma_{90} \sim 10^{-4} - 10^{-2}$ encounters per Myr. For purposes of this discussion, we take the encounter rate to be $\Gamma_{90} = 10^{-3} \text{ Myr}^{-1}$. Over the fiducial timescale of 10 Myr required for planet formation (and observed disk lifetimes), the probability of such a close encounter is low, with odds of only about 1 in 100. Even in more interactive clusters, the odds are only 1 in 10. Although the interaction rates can vary with cluster properties, these results suggest that the early solar nebula is unlikely to have been truncated so severely that giant planet formation is compromised.

Recent observations have begun to constrain the form of the surface density for typical circumstellar disks. For example, one study finds that disks in the Rho Ophiuchus star forming region have surface densities of the approximate form $\Sigma \sim r^{-p} \exp[-r/r_0]$, where the scale $r_0 = 20 - 200$ AU (Andrews et al. 2009; see also Isella et al. 2009). Although preliminary, these results suggest that unperturbed disks might have edges that are softer than the edge structure inferred for the solar nebula (Section 2.5). For example, in our Solar System the observed Kuiper Belt has a mass of $\sim 0.08 M_E$ (Luu & Jewitt 2002); if we augment this mass by a factor of 10 for mass loss, and another factor of 100 to add back in the gaseous component, the inferred surface density is smaller than that of the MMSN (at 30 AU) by a factor of ~ 40 . This density contrast occurs abruptly, whereas an exponential fall-off requires 3.7 scale radii r_0 (74 – 740 AU) to produce such a large decrease in surface density. As a result, some type of truncation event may be required to explain the observed (apparent) edge of the Solar System. In addition to close encounters, the nebula can be truncated by photoevaporation, as discussed in the following section. Note that both mechanisms arise from the background environment.

For completeness, we note that the cluster environment can also add mass to the early solar nebula. As the star/disk system orbits through the cluster potential, the nebula can gain mass through Bondi-Hoyle accretion (Throop & Bally 2008). Through this process, the feeding zone of the solar nebula is given by $R_{BH} = 2GM_*/(v^2 + c_s^2)$, where v is the system speed with respect to the cluster and c_s is the sound speed of the background gas. For typical cluster parameters, the rate of mass accretion $\dot{M} = \pi R_{BH}^2 \rho v$ falls in the range $\dot{M} = 10^{-8} - 10^{-9} M_\odot \text{ yr}^{-1}$. Since gas is typically retained in these clusters for only 3 – 5 Myr (Gutermuth et al. 2009, Allen et al. 2007), the amount of mass added to the disk is expected to fall in the range $(\Delta M)_d \approx 0.003 - 0.05 M_\odot$. Under favorable circumstances, the cluster environment can thus provide the early solar nebula with a mass comparable to the MMSN.

4.4. Disruption of Planetary Orbits

After the planets have formed, and disk truncation is no longer an issue, the planetary orbits are susceptible to disruption. As outlined in Section 2, the orbits of the giant planets in our Solar System are remarkably well-ordered, with low eccentricities and a narrow spread in inclination angle. Although the Solar System would not be seriously compromised if the eccentricities or inclination angles were somewhat higher, we can use these properties to constrain possible interactions between the early Solar System and other stars in its birth cluster. If we let $\langle\sigma\rangle_{ss}$ denote the cross section for disrupting the orbits of the giant planets, this constraint can be written in the general form

$$\int n_* \langle\sigma\rangle_{ss} v dt < 1, \quad (15)$$

where the n_* is the density of passing stars, v is the relative speed, and the integral is taken over the time spent in the birth cluster. Note that additional interactions could, in principle, take place after the Solar System leaves its birth cluster. However, the density of passing stars is lower and the interaction cross sections are smaller (because of the higher relative velocities), and these trends more than compensate for the longer available time.

To evaluate the scattering constraint of equation (15), we consider the Solar System to be “disrupted” if the eccentricities of the giant planet orbits are doubled, or if the spread in their inclination angles is doubled. Notice that this level of disruption is not severe, in that the Solar System could have functioned with larger orbital eccentricities or inclination angles. However, the well-ordered nature of the current planetary orbits shows that such disruption did not in fact take place and we can use this property to place limits on the dynamical history of the Solar System (in the absence of a strong damping mechanism for orbital eccentricity and inclination).

The cross sections for planetary disruption has been calculated through an extensive series of Monte Carlo simulations (Adams & Laughlin 2001; see also Heggie & Rasio 1996, Bonnell et al. 2001, Adams et al. 2006, Malmberg & Davies 2009, Spurzem et al. 2009). In these calculations, we consider the reduced Solar System consisting of the four giant planets and the Sun, where the planets have their measured masses and semi-major axes, but zero eccentricity, and all orbits lie in the same plane. These solar systems are then subjected to fly-by encounters with passing binary stars, where the binary properties, the parameters of the encounter (e.g., impact parameter), and the phases of the planetary orbits are sampled according to a Monte Carlo scheme. The results of these simulations are then used to construct the cross sections for varying levels of solar system disruption.

Figure 1 shows the cross sections for impulsively increasing the eccentricities of the four

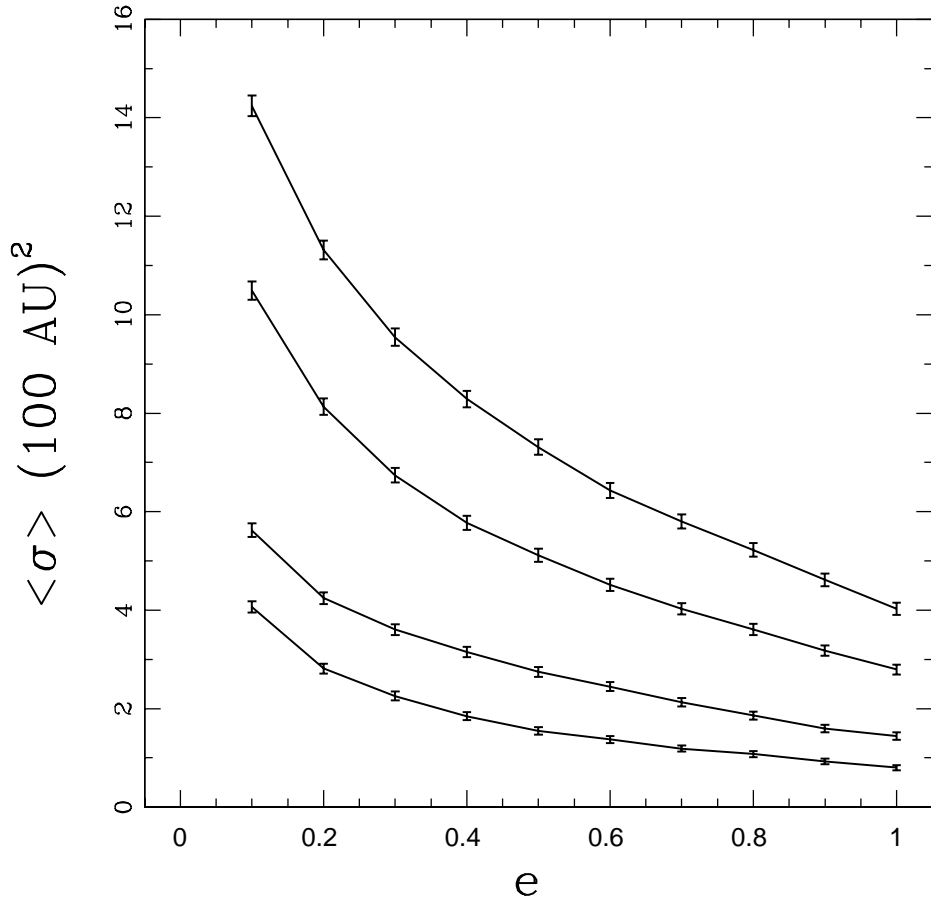


Fig. 1.— Cross sections for disrupting the Solar System through close encounters with passing binary stars. The cross sections are given here for increasing the eccentricity of each planet to a given value e , presented here as a function of eccentricity e . The four curves correspond to the four giant planets from Neptune (top) to Jupiter (bottom). The error bars show the uncertainty due to incomplete sampling in the Monte Carlo procedure (adapted from Adams & Laughlin 2001).

giant planets, given here as a function of eccentricity. The cross section for increasing the eccentricity beyond unity (right side of the figure) corresponds to ejection of the given planet. The cross section for disrupting the solar system (according to the criteria outlined above) takes the value

$$\langle\sigma\rangle_{ss} \approx 160,000(\text{AU})^2 \approx 4 \times 10^{-6}(\text{pc})^2. \quad (16)$$

This cross section corresponds to a distance of closest approach $b \sim 225$ AU.

In recent models of the early Solar System, the giant planets can form in a more compact configuration and then slowly migrate outwards (Tsiganis et al. 2005). Although the tighter orbits could result in a somewhat smaller initial cross section, the difference is small (only a factor of $\sim 2/3$ since the cross sections tend to scale linearly with the outermost semimajor axis; Adams & Laughlin 2001). In addition, eccentricity increases in such a compact configuration can lead to more disruption in subsequent evolution (Malmberg et al. 2007). As a result, equation (16) provides a good working estimate for the disruption cross section.

To interpret this result, we first note that the dynamical speed v within these clusters is typically $v \sim 1 \text{ km s}^{-1} \approx 1 \text{ pc Myr}^{-1}$. If we write the number density of stars n_* in units of pc^{-3} and the time t in Myr, the constraint from the required survival of planetary orbits takes the form

$$\int n_* dt < 250,000 \text{ Myr pc}^{-3}. \quad (17)$$

This constraint shows that even for a relatively high density in the star cluster, say $n_* \sim 1000 \text{ pc}^{-3}$, the Solar System can survive for ~ 250 Myr before disruptions become likely. A similar constraint follows from requiring that the inclination angles of the orbits of Neptune and Uranus are not overly perturbed by passing stars (Gaidos 1995). Note that these (long) timescales can only be realized if the Sun forms within a long-lived cluster, which occurs for about 10 percent of the stellar population.

4.5. Smaller Solar System Bodies

The discovery of an extended scattered disk in the Solar System (Gladman et al. 2002), including the trans-Neptunian object Sedna (Brown et al. 2004), could represent additional evidence for scattering interactions between our Solar System and passing stars. The orbit of Sedna has a large eccentricity ($e \approx 0.84$) with perihelion $p = a(1 - e) \approx 70$ AU. This orbit is thus rather unusual among solar system bodies. Recent numerical studies have shown that this orbit can be produced by a close encounter with a passing star. In one model, Sedna initially resides in the scattered disk and has its perihelion lifted by the encounter (Morbidelli & Levison 2004; Brasser et al. 2006); in another model, the encounter scatters

Sedna from the Kuiper belt into its observed eccentric orbit (Kenyon & Bromley 2004). The required impact parameter for such a collision lies in the range $b \approx 400 - 800$ AU. A close encounter at approximately this distance could also help account for the observed edge of the Kuiper Belt at $r \sim 50$ AU. However, it is difficult to produce a clean edge with a distant fly-by encounter, so that explaining the observed edge would indicate a somewhat closer encounter with approach distance $b = 200 - 300$ AU (see Levison et al. 2004, Kenyon & Bromley 2004, Adams & Laughlin 2001). As outlined in Section 4.1, a typical solar system in a typical cluster is expected to experience about one such close encounter over a time span of 10 Myr. The finding that our Solar System requires (of order) one such encounter is thus consistent with the idea that the Sun formed within a moderate-sized cluster. More specifically, requiring at least one encounter with $b \leq 400$ AU implies that $\int n_* dt \geq 80,000$ Myr pc⁻³ (compare with equation [17]). Meeting this constraint is more likely if the Sun forms within a gravitationally bound cluster, which occurs about 10 percent of the time.

We also note that any stellar encounter that led to the creation of an effective edge to the Kuiper Belt must occur sufficiently early in the Solar System’s evolution. If the encounter takes place more than 10 Myr after the Oort cloud begins forming, either the scattered disk contains too many bodies or the Oort cloud is compromised (Levison et al. 2004).

Before leaving this section, we note that solar systems can eject a large number of rocky bodies during their early phases of evolution. Although this rocky material represents a small fraction of the total mass in solids, about 10 percent, the number of rocks is expected to be large, perhaps $N_R \sim 10^{16}$ bodies with mass $m > 10$ kg. Some fraction of this ejecta remains bound to the cluster and can be captured by other solar systems residing in the birth aggregate (Adams & Spergel 2005, Belbruno et al. 2008). The cross section for rock capture by binary systems is also large, at least $\langle \sigma \rangle \sim (200 \text{ AU})^2$ for the typical velocity dispersions of clusters. With these parameters, every solar system in a cluster can share rocks with every other solar system in the same cluster. One implication of the Sun forming in a cluster is that the Solar System is likely to contain rocks that originated in many other solar systems (perhaps thousands).

5. CONSTRAINTS FROM RADIATION FIELDS

5.1. Radiative Processes in Embedded Clusters

In cluster environments, the ultraviolet (UV) radiation provided by the background often dominates that provided by the central star. Such energetic radiation leads to photo-evaporation of circumstellar disks and hence loss of planet forming potential. If our Solar

System formed within such a cluster, the outer edges of the early solar nebula could be truncated by evaporation. As outlined above, the nebula extended out to at least $r \sim 30$ AU, near the current semi-major axis of Neptune’s orbit. The solar birth cluster is thus constrained — the background radiation must be weak enough to allow gas to survive in the solar nebula at radii $r \leq 30$ AU.

Two types of radiation are important in this context: Ionizing photons with $E_\gamma = h\nu \geq 13.6$ eV, known as EUV radiation, are most efficient at driving photoevaporation (on a per photon basis). The other radiation band of interest, known as FUV, corresponds to the next lower range of energy, where $6 \text{ eV} \leq h\nu < 13.6$ eV. In the largest clusters, EUV radiation is generally the most important. However, EUV radiation is primarily emitted by the largest stars, spectral type OB, which are rare. As a result, in moderate-sized clusters, the photoevaporation process due to external radiation is often dominated by FUV radiation (Hollenbach et al. 1994, Johnstone et al. 1998, Störzer & Hollenbach 1999, Armitage 2000).

5.2. Distribution of UV Radiation Fields

Clusters provide a wide range of possible UV fields that can affect forming solar systems. The most extreme environments are too hostile for planet formation to take place. As a result, our own planetary system is constrained to have formed in the presence of more moderate radiation fields.

Specification of the radiation fields in clusters involves three distributions: First, clusters come in different membership sizes N , so the distribution of clusters df_c/dN comes into play (see Section 3.1). Second, for a fixed value of N , different realizations of the stellar IMF (N times per cluster) lead to a distribution of total UV luminosities for clusters with a fixed membership size N . Finally, photoevaporation depends on UV flux, rather than UV luminosity, and the flux depends on the position of the target solar system within the cluster. Photoevaporation thus depends on the distribution of radial positions of the stars within their cluster, and this distribution is related to the mass profile of the cluster.

If the stellar IMF is fully sampled, the UV luminosity can be characterized by its mean value (where the meaning of being fully sampled is clarified below). Here UV refers to either the EUV or the FUV band. We thus define

$$\langle L_{UV} \rangle_* \equiv \int_0^\infty L_{UV}(m) \frac{dN_*}{dm} dm, \quad (18)$$

where the stellar IMF dN_*/dm vanishes for masses above the upper cutoff $m > m_\infty$ and below the brown dwarf limit $m < m_{min}$. This expectation value is normalized so that $\langle L_{UV} \rangle_*$

corresponds to the mean UV luminosity per star. This quantity is defined once the stellar IMF is specified (assuming that stellar structure models adequately determine the UV fluxes for a given mass). Since the UV luminosity is dominated by the high mass stars, and these objects evolve to the main sequence quickly, we can use stellar configurations on the zero-age main sequence to evaluate this expectation value. For the usual IMF (slope $\gamma = 2.35$, $m_\infty = 100 - 120$), these mean values are $\langle L_{FUV} \rangle_* \approx 1.3 \times 10^{36}$ erg s⁻¹ and $\langle L_{EUV} \rangle_* \approx 9.3 \times 10^{35}$ erg s⁻¹ (Armitage 2000, Fatuzzo & Adams 2008).

To start, we ignore the fact that the UV luminosity in a cluster will have a fairly wide distribution. The expectation value of the UV luminosity for a cluster of membership size N is given by

$$L_{UV}(N) = N \langle L_{UV} \rangle_*, \quad (19)$$

where the subscript UV refers to either the FUV or EUV wavelength band. In the limit of large N , this expectation value provides a good estimate, and the distribution of luminosity about this mean value approaches a gaussian form due to the central limit theorem. In practice, however, convergence is extremely slow and the moderate-sized clusters of interest display large departures from gaussianity. In particular, the median values of the distributions are significantly below the mean (Fatuzzo & Adams 2008) and the distributions are wide. For example, the standard deviation of the distribution of L_{FUV} is larger than the mean value (given by equation [19]) for $N \leq 700$. Similarly, the standard deviation of the L_{EUV} distribution is wider than the mean for $N \leq 1400$. These results indicate that the cluster to cluster variation (for fixed N) is important for moderate-sized systems. More specifically, for the solar neighborhood cluster sample (Lada & Lada 2003, Porras et al. 2003), half of the stars are found in clusters with $N \leq 300$; and $\sim 80\%$ (90%) of the stars are found in clusters with $N \leq 700$ (1400).

The above considerations describe the expected values of UV luminosities for cluster environments. To understand the possible impact on the early Solar System, however, we must determine the distribution of UV fluxes. We focus here on the case of the FUV flux distribution; the EUV fluxes can be treated in similar fashion. This overall distribution depends on three input distributions: First, the clusters themselves come in a variety of membership sizes N . Second, for a given N , each cluster will sample the stellar IMF differently, and the resulting sampling will give rise to a distribution of UV luminosity for fixed N (see above). Finally, for a given cluster size N and realization of the IMF, the distribution of radial positions within the cluster produces a corresponding distribution of UV fluxes. The resulting composite FUV flux distribution, for the collection of clusters found in the solar neighborhood, is shown in Figure 2. The FUV fluxes are expressed in units G_0 , defined so that $G_0 = 1$ corresponds to the value $F_{FUV} = 1.6 \times 10^{-3}$ erg s⁻¹ cm⁻² (close to the value appropriate for the interstellar medium; see Habing 1968). The cluster environment thus

produces FUV radiation fluxes that are thousands of times more intense than in the field. Similar results hold for the case of EUV radiation (Armitage 2000).

We can gain further insight by considering the expected flux levels within clusters with given membership N (as a function of N). The mean luminosities for both FUV and EUV radiation are given above. For clusters with exceptionally large N , the expected luminosity is close to mean; for more moderate clusters, however, the median luminosity is smaller than the mean by a factor $f_m \approx 0.8$ (Fatuzzo & Adams 2008). To estimate the flux, we must specify the radial location, which we take to be the expectation value $r = \langle r \rangle = 2R/3$, where R is the cluster radius (see equation [7]). The expected UV flux is thus given by

$$F_{UV} \approx \frac{f_m N \langle L_{UV} \rangle_*}{4\pi r^2} = \frac{9f_m N_0 \langle L_{UV} \rangle_*}{16\pi R_0^2} \left(\frac{N}{N_0} \right)^{1-2\alpha}. \quad (20)$$

The fiducial flux level $F_{UV} = 9f_m N_0 \langle L_{UV} \rangle_* / 16\pi R_0^2$ is thus $F_{FUV} \approx 5.8 \text{ erg s}^{-1} \text{ cm}^{-2}$ ($G_0 \approx 3600$) for FUV, and $F_{EUV} \approx 4.2 \text{ erg s}^{-1} \text{ cm}^{-2}$ ($2 \times 10^{11} \text{ photons s}^{-1} \text{ cm}^{-2}$) for EUV radiation.

As outlined below, these flux levels (especially for FUV) are intense enough to affect the early solar nebula. Since the index $\alpha \sim 1/2$, as least for clusters in the solar neighborhood, these fiducial flux levels are slowly varying with cluster membership size. On the other hand, in the regime of large N , the cluster radius index $\alpha = 1/4 - 1/3$, so that the flux levels are higher. In addition, the inner portions of large clusters produce much stronger radiative fluxes. However, the solar nebula can survive in such large clusters, provided that the Sun spends much of its time in the outer regions. This point is reinforced in subsequent sections.

5.3. Photoevaporation of Disks

When a disk is exposed to external UV radiation, the gas can be heated to sufficiently high temperatures to drive an evaporative flow. This process defines a critical fiducial length scale, the radius at which the sound speed of the heated gas exceeds the escape speed from the Sun:

$$r_g = \frac{GM_*}{a_S^2} = \frac{GM_* \langle \mu \rangle}{kT} \approx 100 \text{ AU} \left(\frac{T}{1000 \text{ K}} \right)^{-1}, \quad (21)$$

where we have used the mass of the Sun. If EUV photons can penetrate the outward flow with sufficient flux, they can heat the gas to temperatures $T \sim 10^4 \text{ K}$. On the other hand, FUV photons generally heat the gas to lower temperatures with $T = 100 - 3000 \text{ K}$. The delineation of the regimes for which EUV and FUV radiation dominates the mass loss is complicated (Johnstone et al. 1998, Störzer & Hollenbach 1999, Armitage 2000, Adams et al. 2004, Clarke 2007, Ercolano et al. 2009). A brief overview is presented below.

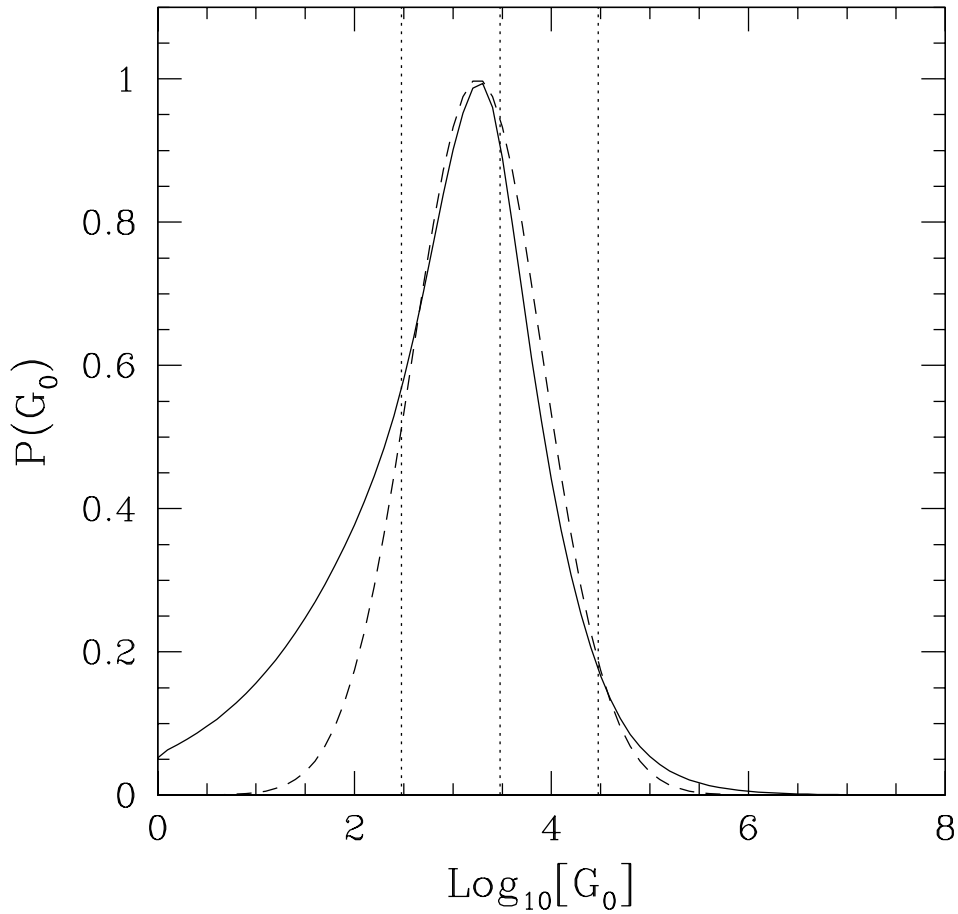


Fig. 2.— Distribution of FUV radiation fluxes for the collection of young embedded clusters in the solar neighborhood. This distribution is obtained by convolving the distribution of cluster membership sizes N , the distribution of FUV luminosities for fixed N due to different sampling of the stellar initial mass function, and the distribution of radial positions with the clusters. The three vertical lines delimit benchmark values of $G_0 = 300$, 3000 , and 30000 (adapted from Adams et al. 2006).

For EUV radiation, the mass loss rate from a disk due to photoevaporation can be written in the approximate form

$$\dot{M} \approx (9 \times 10^{-8} M_{\odot} \text{ yr}^{-1}) \left(\frac{\Phi}{10^{49} \text{ s}^{-1}} \right)^{1/2} \left(\frac{d}{10^{17} \text{ cm}} \right)^{-1} \left(\frac{r_d}{30 \text{ AU}} \right)^{3/2}, \quad (22)$$

where Φ is the EUV photon luminosity, d is the distance of the solar system to the cluster center, and r_d is the disk radius (Shu et al. 1993, Johnstone et al. 1998). The mass outflow rate thus scales according to $\dot{M} \propto F_{EUV}^{1/2}$, where F_{EUV} is the flux of EUV photons from the cluster (keep in mind that the EUV is assumed to be generated by massive stars at the cluster center).

Consider a typical cluster in the solar neighborhood, with $N = 300$ and radius $R = 1$ pc. For a standard stellar IMF, the system is expected to have 1 or 2 stars with mass $M_* > 10M_{\odot}$. If we consider a typical solar system to lie at a distance $d = R/2$, the EUV flux is $F_{EUV} = \Phi/(4\pi d^2) \approx 4.3 \times 10^{11}$ photons $\text{s}^{-1} \text{ cm}^{-2}$, the mass outflow rate from equation (22) becomes $\dot{M} \approx 6.8 \times 10^{-9} M_{\odot} \text{ yr}^{-1}$. This evaporation rate can be converted into a timescale by assuming a starting disk mass, which we take to be $M_d = 0.05 M_{\odot}$ (comparable to the MMSN). The resulting fiducial timescale for evaporation (with disk radius $r_d = 30$ AU) is $t \approx 147$ Myr, longer than typical disk lifetimes. A solar system at a typical location in moderate-sized cluster is not greatly affected by photoevaporation from EUV radiation. Larger EUV fluxes can disrupt the disk.

To illustrate these trends, Figure 3 plots the timescale for disk evaporation as a function of outer disk radius. We assume that the disk mass scales with disk radius according to $M_d \propto r_d^{1/2}$, as expected for surface density $\Sigma \propto r^{-3/2}$. The five curves correspond to varying EUV fluxes from $F_{EUV} = 10^{11}$ to 10^{15} photons $\text{s}^{-1} \text{ cm}^{-2}$. The lowest flux corresponds to that expected for a solar system living at the edge of a moderate-sized cluster with $N = 300$. The evaporation timescales become problematic (where the solar nebula is evaporated in 10 Myr at radius 30 AU) only when the EUV flux is ~ 1000 times the nominal value. Note that for less steep surface density profiles (e.g., $\Sigma \propto r^{-1}$), the evaporation time scales are even longer for $r_d < 30$ AU.

Given that EUV radiation becomes important only in extreme regimes of parameter space, we now turn to the effects of FUV radiation. As shown in Figure 2, clusters in the solar neighborhood provide a well-defined distribution of FUV fluxes, with typical values in the range $G_0 = 1000$ to $10,000$. For comparison, if we use the expectation value for the FUV luminosity of a cluster with $N = 300$ (see equation [19]), the expected flux at $R = 1$ pc corresponds to $G_0 \approx 2000$.

Figure 4 shows the expected evaporation times for a solar nebula heated by external

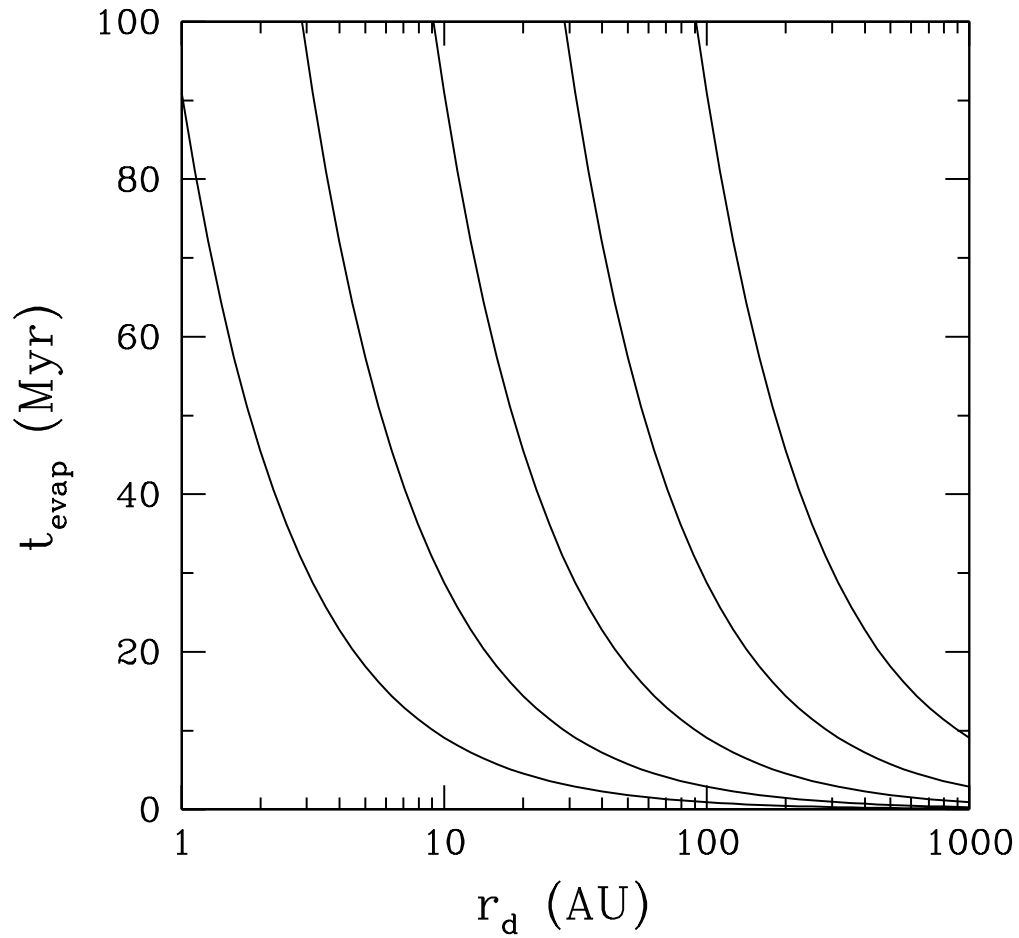


Fig. 3.— Photoevaporation timescales for the solar nebula as a function of disk radius r_d for varying external EUV fluxes. The five curves correspond to EUV fluxes $F_{\text{EUV}} = 10^{11}$, 10^{12} , 10^{13} , 10^{14} , and 10^{15} photons $\text{s}^{-1} \text{cm}^{-2}$ (increasing from right to left). Typically expected flux levels correspond to the lower values (see text).

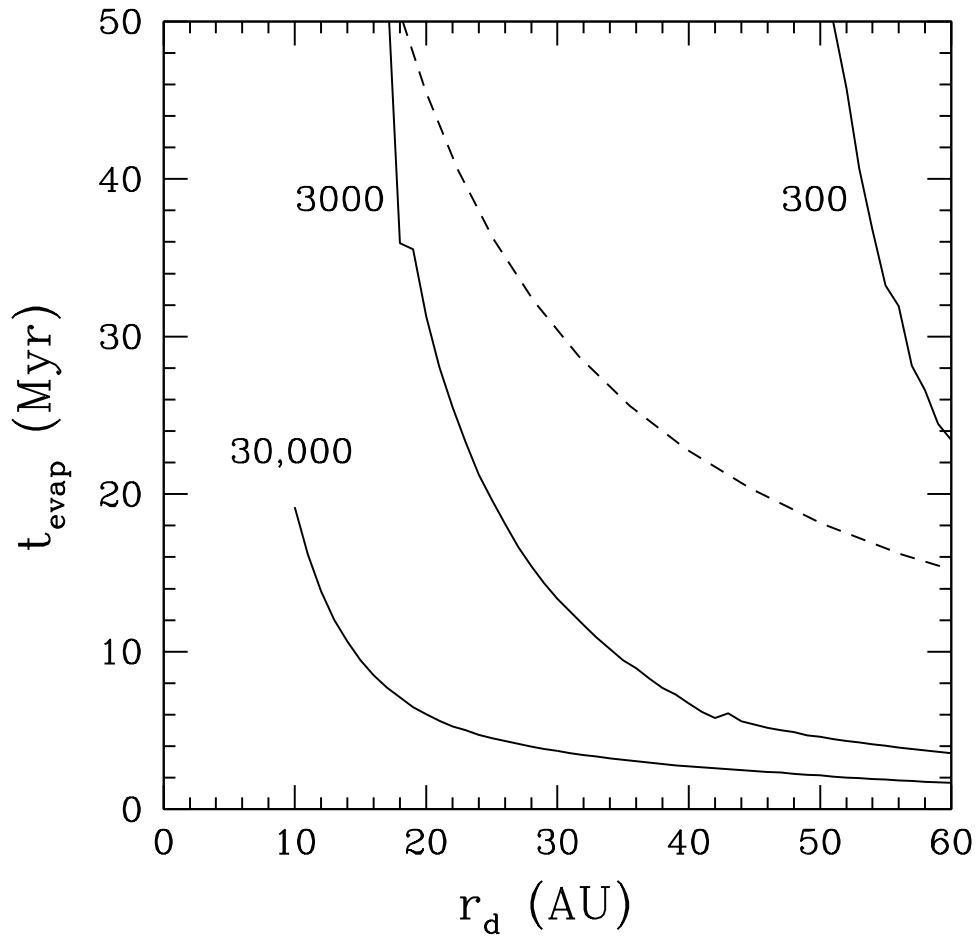


Fig. 4.— Photoevaporation timescales for the solar nebula as a function of disk radius r_d for varying external FUV fluxes. The three solid curves correspond to FUV fluxes with $G = 300$, 3000, and 30,000 as labeled. The dashed curve shows the timescale for EUV evaporation with EUV flux $F_{\text{EUV}} = 10^{13}$ photons $\text{s}^{-1} \text{cm}^{-2}$, which corresponds to 100 times the “typical value” (see text).

FUV radiation (the mass loss rates are taken from Adams et al. 2004, which uses the heating/cooling formalism from Kaufman et al. 1999). The three solid curves correspond to the benchmark values of FUV flux with $G_0 = 300, 3000, \text{ and } 30,000$. Note that this figure is plotted on a smaller scale than that used to illustrate the effects of EUV radiation (compare with Figure 3) because the expected FUV radiation can evaporate the solar nebula down to smaller radii. For comparison, Figure 4 also shows the timescales for evaporation with an EUV flux F_{EUV} that is 100 times larger than the typically expected value. These high EUV flux levels can be realized for solar systems located at distances $d \sim R/10$, i.e., in the central cores of the clusters. Note that expected FUV fluxes ($G_0 \sim 3000$) can evaporate the solar nebula at $r_d = 30$ AU over a timescale of 15 Myr. Since giant planets are expected to form on somewhat shorter timescales (3 – 10 Myr, Lissauer & Stevenson 2007), the solar nebula is relatively safe. For more extreme fluxes with $G_0 = 30,000$, only the outer 20 AU of the solar nebula can survive for 6 Myr. Thus, survival of the early solar nebula, out to $r_d \sim 30$ AU, requires that the FUV flux cannot exceed an intermediate value, i.e., $G_0 \leq 10^4$.

For completeness we note that Neptune and Uranus are ice giants, rather than gas giant planets like Jupiter and Saturn. The relatively low gas content in these bodies could imply that the early solar nebula did in fact experience some photoevaporation near $r = 30$ AU. If this were the case, FUV flux levels near $G_0 \sim 10^4$ would be required. Alternatively, these bodies could form over long timescales such that less gas is present.

Observations of circumstellar disks in the Orion Trapezium Cluster, a nearby region containing high mass stars and intense radiation fields, indicate that the fraction of systems containing at least a MMSN within $r = 60$ AU is ~ 12 percent (Mann & Williams 2009). This percentage is comparable to that in Taurus, a region with no high mass stars and little background radiation. Taken together, these observational results argue that cluster environments provide relatively modest constraints on the mass available for planet formation, a conclusion consistent with the theoretical considerations outlined above.

5.4. Ionization and Other Effects

Cluster environments provide important sources of ionization for forming and newly formed solar systems. These sources include ionizing EUV radiation, X-rays, and cosmic rays. The distributions of EUV fluxes are described in Section 5.2 (see also Figure 3). For larger clusters with membership $N \geq 100$, the background cluster environment provides more ionizing photons to the solar nebula than the early Sun itself (Adams & Myers 2001). Most of the external EUV photons are captured by the outer disk, whereas most of the Solar EUV photons are intercepted by the inner disk; the relative importance of the two ionization

sources thus varies with radial position.

The case of X-ray radiation, with photon energy $h\nu \geq 0.1$ keV, is similar: The typical X-ray luminosity from young stars falls in the range $L_X \approx 10^{29} - 10^{32}$ erg s⁻¹ for stellar masses in the range $M_* = 0.3 - 7 M_\odot$ (Preibisch et al. 2005). For larger stars, $L_X \approx 10^{-6} L_*$. With these luminosities, X-rays provide fewer ionizing photons than the EUV band. However, the EUV radiation is more easily absorbed, so that both sources of radiation must generally be considered (see Gorti & Hollenbach 2009, Ercolano et al. 2009).

Cosmic rays provide an important source of ionization, especially deep within molecular clouds where star formation takes place and where UV radiation can be shielded. Since supernovae are the source of cosmic rays, and since they generally explode within or near molecular clouds, cosmic ray fluxes can be enhanced relative to their standard values in the interstellar medium. Further, since the clouds are supported (at least in part) by magnetic fields, which act to retain cosmic rays within the clouds, substantial enhancements are possible (Fatuzzo et al. 2006). The short-lived radio isotopes (discussed in the following section) also provide significant sources of ionization, with ²⁶Al being one of the most efficient (Umebayashi & Nakano 2009).

Ionization levels are important for star formation and planet formation. In the early phases of star formation, molecular cloud cores are supported, in part, by magnetic fields. Although the relative importance of magnetic diffusion and turbulence is currently under debate (compare Shu et al. 1987 with McKee & Ostriker 2007), loss of magnetic flux is necessary for stars to form. Increasing the ionization increases the coupling between the field and the largely neutral gas, and thereby decreases the ability of magnetic fields to diffuse away. The density of ions ρ_i in molecular clouds is given by $\rho_i = \mathcal{C} \rho_n^{1/2}$, where ρ_n is the density of neutral atoms; the constant $\mathcal{C} \propto \zeta^{1/2}$, where ζ is the flux of cosmic rays. The effective diffusion constant D for magnetic flux loss is then given by

$$D = \frac{v_A^2}{\gamma_{in} \mathcal{C} \rho} \propto \zeta^{-1/2}, \quad (23)$$

where v_A is the Alfvén speed and γ_{in} is the drag coefficient between ions and neutrals (Shu 1992).

Ionizing radiation in clusters also influences disk accretion, which is driven by an effective viscosity resulting from turbulence. This turbulence, in turn, is thought to be driven by MHD effects such as the magneto-rotational instability (MRI, Balbus & Hawley 1991). The presence of MRI and hence disk accretion requires that the ionization fraction in the disk is high enough for the gas to be well-coupled to the magnetic field. The inner disk can be ionized by collisions, and the outer disk can be ionized by cosmic rays. At intermediate radii,

however, the disk can have dead zones where ionization levels are too low (Gammie 1996). Enhanced ionization in clusters thus acts to make more of the disk support MRI. Thus, one consequence of the Sun forming in a cluster is that disk accretion could be enhanced relative to the rates it would have experienced in isolation.

Finally, we note that strong radiation fields can produce chemical signatures in forming solar systems. Our own solar system displays an oxygen isotopic anomaly that can be explained if the Sun formed in the presence of intense FUV radiation fields. In one scenario, ultraviolet radiation produces selective photodissociation of CO within the collapsing protostellar envelope of the forming Sun (Lee et al. 2008); in an alternate scenario, the isotope selective photodissociation occurs at the surface of the early solar nebula (Lyons & Young 2005). Since a range of oxygen anomalies are possible, given current measurements, the required FUV flux is not well determined. Future observations will provide much tighter constraints.

6. CONSTRAINTS FROM NUCLEAR ENRICHMENT

6.1. External Enrichment through Supernovae

As outlined in Section 2.7, meteoritic evidence implies that the early solar nebula contained significant quantities of radioactive nuclei with half-lives shorter than 10 Myr (see Table I). Supernovae provide one possible source for these short-lived ratio isotopes. The idea of a supernova explosion associated with the formation of the Solar System has a long history. One of the first isotopes to be considered was ^{26}Al , which has a half-life of only 0.72 Myr. To explain the presence of ^{26}Al , Cameron & Truran (1977) suggested that supernova ejecta containing the short-lived species could be incorporated into the dense core that formed the Solar System (note that asymptotic giant branch stars can also produce ^{26}Al — see Section 6.5). This idea of external enrichment has been expanded upon as additional nuclear species were discovered in meteorites (Table I). In particular, the isotope ^{60}Fe is extremely difficult to produce through spallation reactions, but is naturally produced by stellar nucleosynthesis. As a result, a number of authors have presented scenarios for supernova enrichment of the early solar nebula (including Cameron et al. 1995, Boss & Foster 1998, Goswami & Vanhala 2000, Looney et al. 2006, Williams & Gaidos 2007, and many others; see also references therein). Although a range of progenitor masses M_* are possible, and no mass scale produces perfect abundances, these studies suggest that stars with $M_* \approx 25M_\odot$ provide the best ensemble of short-lived radioactive nuclei. This section outlines the basic requirements necessary for supernova enrichment to take place, as well as the corresponding constraints on the solar birth environment. Some of the difficulties faced by this scenario

are also discussed.

One needs a moderately large cluster to provide a supernova from a sufficiently massive progenitor star. The stellar mass distribution of equation (1) indicates that the probability that a star has mass (in solar units) greater than a mass scale m_0 is given by the expression

$$P(m \geq m_0) = \mathcal{F}_1 m_0^{-\gamma} \left[1 - \left(\frac{m_0}{m_\infty} \right)^\gamma \right], \quad (24)$$

where m_∞ is the maximum stellar mass. For example, the probability P_{25} that a star has at least the benchmark progenitor mass for supernovae enrichment, $m_0 = 25$, is given by $P_{25} \approx 0.00084$ (where we have used standard values $\mathcal{F}_1 = 0.12$, $\gamma = 1.5$, and $m_\infty = 100$). The probability $\mathcal{P}_N(m > m_0)$ that a system of N stars contains at least one star greater than mass m_0 is then given by

$$\mathcal{P}_N(m > m_0) = 1 - [1 - P(m > m_0)]^N. \quad (25)$$

Throughout this analysis, we assume that high mass stars, specifically those that can be progenitors of the supernova that enriched the early solar nebula, are drawn at random from the IMF, and that this property holds for all cluster sizes N . Although the largest stellar mass in a system could in principle be correlated with cluster membership size N , available data remain consistent with no such correlation, especially for larger clusters (Maschberger & Clarke 2008). The resulting probability distributions for a cluster to produce a high mass progenitor are shown in Figure 5 for stellar masses $m_0 = 10, 25$, and 75 .

We define $N_{50}(m_0)$ to be the cluster membership size that is required for the system to have a 50/50 chance of containing a star with mass $m > m_0$. In general, for mass m_0 , this required cluster size is given by

$$N_{50} \approx \frac{(\ln 2) m_0^\gamma}{\mathcal{F}_1 [1 - (m_0/m_\infty)^\gamma]}. \quad (26)$$

The cluster size required to have a 50/50 chance of containing a 25 solar mass star is thus $N_{50} \approx 825$. For comparison, the cluster size required to have a 50/50 chance of realizing a 75 solar mass star is $N_{50} \approx 10,700$. Provided that the progenitor mass m_0 is not near the upper limit m_∞ , equation (26) simplifies to the approximate form $N_{50} \approx 6 m_0^{3/2}$, where we have inserted typical values for the remaining parameters. Keep in mind that different progenitor masses have different main sequence lifetimes, and that timing is also important for successful nuclear enrichment (see the discussion below).

The distance d from the supernova progenitor to the early solar nebula must be close enough to provide the observed abundances of radioactive isotopes. The nominal distance

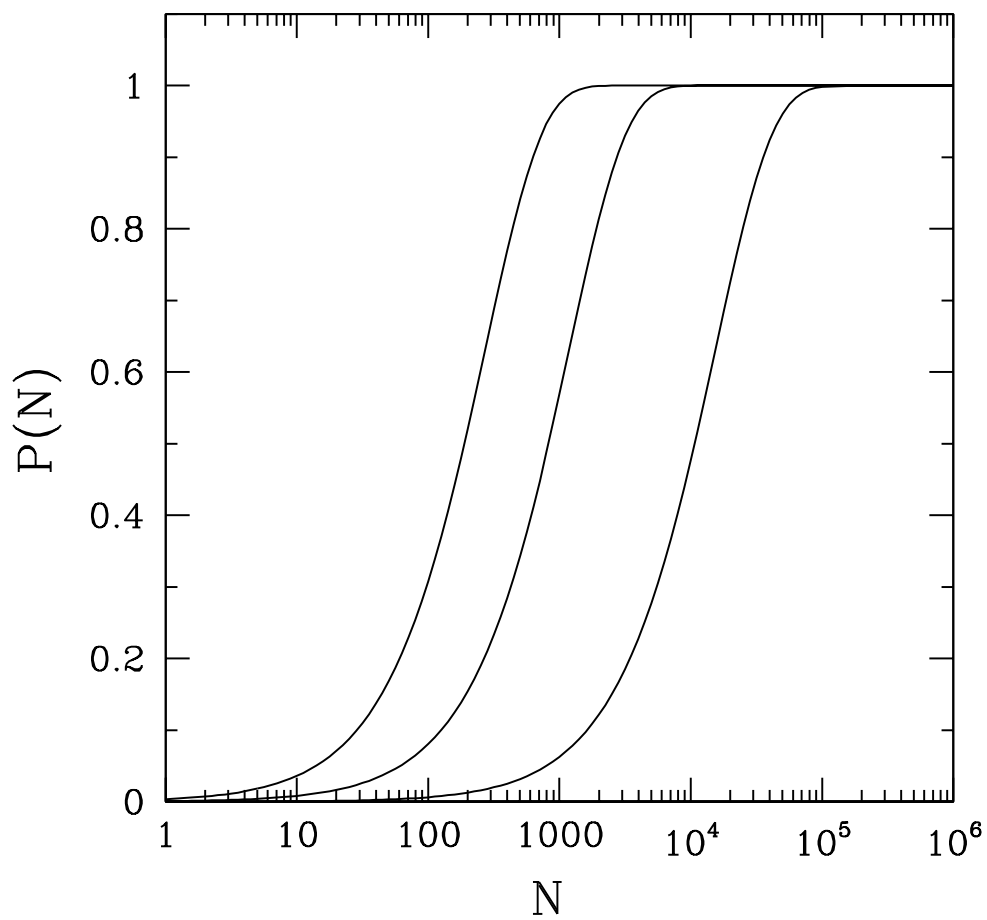


Fig. 5.— Probability for a cluster of membership size N to produce a supernova progenitor of a given mass M_* as a function of N . The three curves show the probability distributions for progenitor masses of $M_* = 10, 25,$ and $75 M_\odot$ (from left to right).

from the supernova explosion to the solar nebula can be estimated by requiring the mass fraction X_j of a given nuclear species to be large enough. This fraction is given by

$$X_j = f_j \frac{M_j}{M_d} \frac{\pi r_d^2}{4\pi d^2}, \quad (27)$$

where M_d is the mass of the solar nebula at the time of enrichment, f_j is the fraction of the material that is absorbed by the nebula, and r_d is its radius (Looney et al. 2006, Ouellette et al. 2007). For example, calculations of radioactive yields by Type II supernovae indicate that such explosions produce $M_{\text{Fe}} = 2.4 - 16 \times 10^{-5} M_\odot$ of ^{60}Fe , where the value depends on the progenitor mass (Rauscher et al. 2002). Using this result and the mass fraction X_{Fe} for ^{60}Fe (see Table I), and parameters of the minimum mass solar nebula ($M_d = 0.05 M_\odot$, $r_d = 30$ AU), we find the required distance to fall in the range $d \approx 0.1 - 0.3$ pc. This estimate assumes that all of the material is accreted by the nebula so that $f_j = 1$; the inclusion of an efficiency factor $f_j \neq 1$ implies an even closer distance. This estimate also assumes that the nebula is facing into the blast; significant inclination angles will also reduce the estimated distance. On the other hand, non-uniform ejecta (clumps) can lead to greater yields and allow for a larger distance. Nonetheless, in order of magnitude, the required distance for sufficient enrichment is $d \sim 0.2$ pc.

On the other hand, a minimum mass solar nebula will be stripped by a supernova blast wave if it lies too close to the explosion. This minimum distance is also estimated to be about 0.2 pc (Chevalier 2000), as outlined below. As a result, there is some tension between the requirement that the supernova is close enough to produce sufficiently high yields of the radio isotopes and yet far enough that the early solar nebula survives.

The early solar nebula can be truncated by a supernova explosion in two ways. When the ram pressure $P_{ram} = (\rho v^2)_{SN}$ of the supernova flow exceeds the force per unit area with which the Sun holds onto the nebular gas, the material is subject to stripping. This second pressure scale is given roughly by $P_\odot \sim GM_*\Sigma/r_d^2$, where Σ is the disk surface density and r_d is the radial location within the disk. For supernovae, the ram pressure $(\rho v^2)_{SN} \approx A_{SN}E_{SN}/r^3$, where $E_{SN} \approx 10^{51}$ erg, r is the distance to the explosion, and the dimensionless parameter A_{SN} is of order unity (Chevalier 2000). The condition for ram pressure stripping thus takes the form

$$A_{SN} \frac{E_{SN}}{r^2} = \frac{GM_*}{r_d^2} \Sigma(r_d). \quad (28)$$

Similarly, the early solar nebula can be destroyed by momentum transfer if the momentum per unit area imparted by the supernova blast wave exceeds the corresponding scale of the star/disk system. This criterion for momentum stripping can be written in the form

$$\frac{M_{ej}v_{SN}}{4\pi r^2} = \left(\frac{2GM_*}{r_d} \right)^{1/2} \Sigma(r_d), \quad (29)$$

where $M_{ej} \approx 1M_{\odot}$ is the mass of the ejecta. The maximum radii of the solar nebula that can survive these two types of stripping processes are shown in Figure 6. The curves in this figures are calculated for a minimum mass solar nebula, and for the values of M_{ej} and E_{SN} given above (note that $v_{SN}^2 = 2E_{SN}/M_{ej}$). In general, ram pressure stripping is more destructive than momentum stripping. These results indicate that the supernova explosion must be farther away than $r = d \sim 0.1$ pc in order for the solar nebula, with outer radius $r_d \approx 30$ AU, to survive intact. Note that recent numerical studies indicate that the solar nebula can survive at even closer distances (Ouellette et al. 2007).

The above considerations show that the early solar nebula must be close enough to the supernova ($d \leq d_2 \approx 0.3$ pc) to receive enough nuclear enrichment, and far enough away ($d \geq d_1 \approx 0.1$ pc) to survive the experience. It is significant that an intermediate range of radii allows for both conditions to be met. However, the probability of the solar nebula residing in this range of radii is relatively low: For example, the radial probability distribution from equation (9) implies that the probability P_d of a star finding itself in the radial range $0.1 \text{ pc} \leq d \leq 0.3 \text{ pc}$ is given by $P_d = 0.08(\text{pc})^2/R^2 \approx 0.02$. The latter numerical value assumes that the cluster radius $R = 2$ pc, a typical value for a moderately large cluster (see equation [7]). One can generalize this result to include cluster density profiles of the form $n_* \propto r^{-p}$ with outer radii given by equation (7):

$$P_d = [(d_2/R_0)^{3-p} - (d_1/R_0)^{3-p}] \left(\frac{N_0}{N} \right)^{\alpha(3-p)}, \quad (30)$$

where $R_0 = 1$ pc and $N_0 = 300$; we expect the indices to fall within the ranges $1 \leq p \leq 2$ and $1/4 \leq \alpha \leq 1/2$. The typical value is thus $P_d \sim$ few percent.

The lifetimes of potential progenitors provide another strong constraint on the supernova enrichment hypothesis. As outlined above, the radio isotope yields work best for progenitor masses $M_* \approx 25M_{\odot}$. Stars with this initial mass spend about 6.7 Myr in their main-sequence hydrogen burning phase, and a total of ~ 7.54 Myr before core collapse (Woosley et al. 2002). These timescales decrease with increasing starting mass: For comparison, stars with initial mass $15 M_{\odot}$ ($75 M_{\odot}$) spend 11.1 Myr (3.16 Myr) on the main sequence and a total of 12.1 Myr (3.64 Myr) before exploding as supernovae. Given that age spreads in young embedded clusters are relatively small, only about 1 – 2 Myr (Hillenbrand 1997), and that most clusters are dispersed in ~ 10 Myr or less (Allen et al. 2007), these progenitor lifetimes are somewhat long for comfort. Nonetheless, a possible solution exists, provided that the massive star forms first and the Sun forms several Myr later. In this case, however, the forming Solar System could be less likely to reside within the required nuclear enrichment zone ($d = 0.1 - 0.3$ pc) due to radiative disruption from the pre-existing progenitor.

In addition to the lifetime issue, the necessity of having a large progenitor star to explain

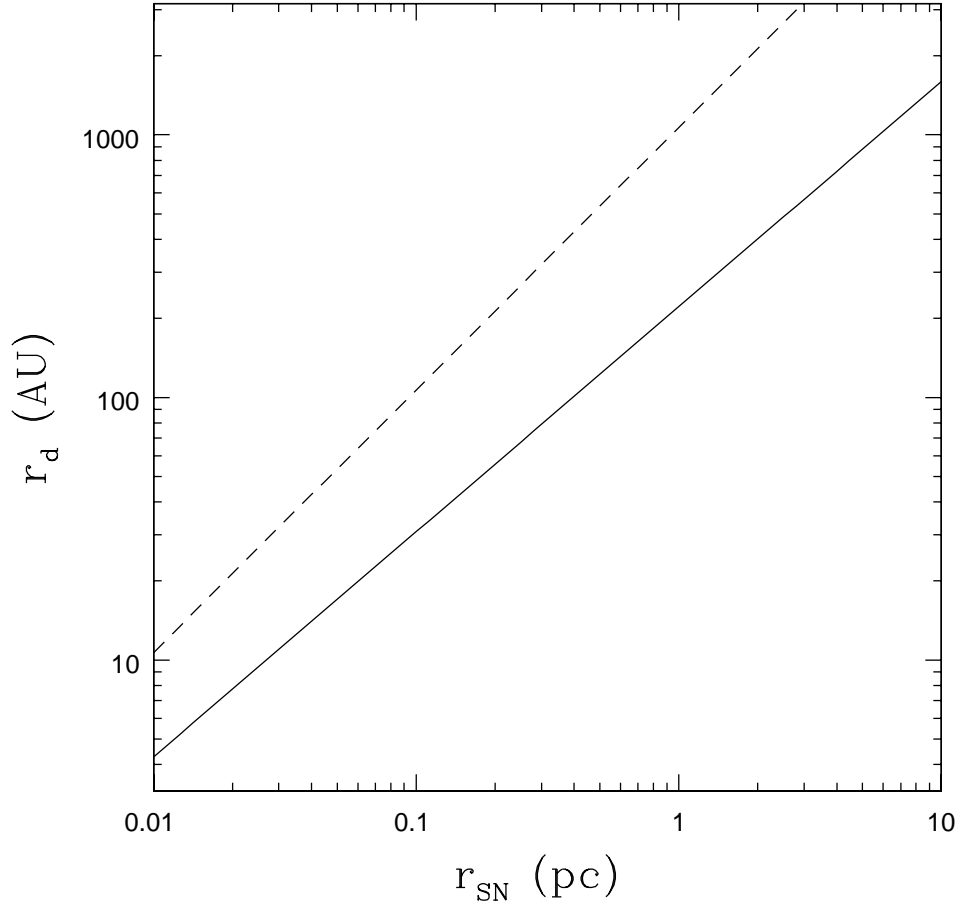


Fig. 6.— Disk radius r_d that can survive a supernova blast wave as a function of the distance r_{SN} from the star/disk system to the explosion. The solid line shows the disk radius that can survive ram pressure stripping; the dashed line shows the disk radius that can survive momentum stripping.

nuclear enrichment introduces another strong constraint. The massive progenitor star will produce large amounts of EUV and FUV radiation, which can readily evaporate the early solar nebula (see Section 5, Gounelle & Meibom 2008). If the Sun spends too much time close to the progenitor, before the explosion, the solar nebula could be compromised. For example, consider a cluster with $N = 1000$ members and let its UV luminosity be given by equation (19); if the solar system orbits at a distance from the center with $d = 0.3$ pc, the expected FUV flux has a value $G_0 \approx 60,000$. This radiation field can readily evaporate the solar nebula, and would remove all gaseous material beyond ~ 10 AU over a time span of 10 Myr (see Figure 4). As a result, there is significant tension between the radiation fields produced by the progenitor and the relatively close proximity required for successful nuclear enrichment. Of course, the Sun could spend much of its time (during the main-sequence phase of the progenitor) in the outer parts of the cluster, where the radiation fields are low. The Sun would then have to enter the central part of the cluster just before the supernova explosion. This timing of events is possible, since most stars spend most of their time outside the inner enrichment zone of a cluster. However, this requirement lowers the odds for supernova enrichment (see also Williams & Gaidos 2007).

6.2. Triggering of Solar System Formation

Two versions of the external enrichment scenario have been proposed. In the first and simplest case, the supernova enriches the Solar System after it has already begun formation. Here, the supernova ejecta are intercepted by the early solar nebula, as discussed above. In the second version, the supernova that enriches the Solar System also triggers the initial collapse of the molecular cloud core that gives rise to the Sun (Cameron & Truran 1977, Vanhala & Boss 2002). In this case, the supernova ejecta are incorporated into the molecular cloud material that subsequently collapses to form the Solar System.

Current observational data suggest that the latter, directly triggered scenario is less likely than the alternative. The cluster environments found in the solar neighborhood (Lada & Lada 2003, Porras et al. 2003, Allen et al. 2007) are generally not influenced by supernovae: Although the data remain incomplete, the spread in ages in these clusters is small, typically less than ~ 1 Myr (Allen et al. 2007); since this timescale is shorter than the main sequence lifetime of supernova progenitors, none of the stars in these cluster systems were triggered to collapse by supernovae exploding within the same cluster. In a similar vein, the statistics of these clusters suggest that the gas is removed, and hence that star formation shuts down, after only 3 – 5 Myr (e.g., Gutermuth et al. 2009, Lada & Lada 2003). This timescale is (again) shorter than the main sequence lifetime of most supernova progenitors

(Section 6.1), so that no gas is expected to be left in the cluster when stellar explosions eventually occur.

For completeness we note that although supernova triggering does not seem to take place within the embedded clusters observed in the solar neighborhood, triggering mechanisms are not completely ruled out. In particular, collapse can be induced, or at least helped along, by ionization fronts driven by massive stars (for further discussion of latter this issue, see Hester & Desch 2005, Snider et al. 2009). In addition, supernovae do in fact shape star formation environments, but their actions take place over time scales (~ 10 Myr) and length scales (many pc) that are larger than those appropriate for star formation within a single cluster — there is an impedance mismatch between supernova triggering and cluster scales.

6.3. Internal Enrichment through Irradiation

Some fraction of the short-lived radio isotopes can be produced by internal processes, i.e., by the forming Sun itself. Note that if all of the observed nuclear species could be produced internally, then nuclear enrichment would not require an external supernova or other source of short-lived isotopes. In that case, the birth environment of the Sun would be decoupled from nuclear considerations. In spite of the progress made over the last decade (Lee et al. 1998, Shang et al. 2000, Shu et al. 2001), it remains difficult for internal processes to explain the entire ensemble of isotopes, so that some supernova enrichment is still (apparently) required. On the other hand, self-enrichment may be required to explain the presence of some nuclear species and is thus likely to contribute to the supply of other isotopes. In this manner, the requirements placed on external sources are made less restrictive.

The leading picture for internal enrichment is generally called the X-wind model (Shu et al. 2004). During the protostellar collapse phase of the early Sun, a wind emerges from the inner portion of the rapidly rotating solar nebula. The Sun and its circumstellar disk are coupled by strong magnetic fields anchored within the star; the disk is also influenced by additional magnetic fields that are dragged in from the original cloud. These fields drive a powerful stellar wind through magnetic/centrifugal effects, and the wind collimates into a narrow jet with a molecular outflow. As rocks enter the launching region of the wind, they are lifted up, heated and irradiated by both photons and energetic particles from the stellar surface, and then thrown outward. Small bodies can be carried out of the Solar System along with the wind, whereas much larger bodies move relatively little and fall near their launching locations. The rocks of intermediate mass, those with sizes in the range 0.2 – 2 mm, fall out of the wind at radii comparable to the present day asteroid belt, where they can be incorporated into meteoritic material (Shang et al. 2000).

This X-wind environment provides both heating of the rocky material that it processes and the production of radioactive nuclear species. Although both processes are important for understanding the properties of our Solar System, the latter has a more direct bearing on the possible birth place of the Sun. In this setting, radio isotopes are produced by energetic particles — essentially cosmic rays — that are released by energetic protostellar flares near the surface of the star. These high energy cosmic rays induce spallation reactions, which, in turn, can synthesize some of the short-lived radioactive isotopes that are thought to be present in the early solar nebula.

In the present day Sun, gradual flares dominate the production of the cosmic rays that can leave the Solar System because these flares operate on open magnetic field lines. Impulsive flares on closed field lines provide more energetic particle displays. In the early Sun, these impulsive flares are thought to dominate (see the discussion of Shang et al. 2000) and create a prolific source of ^3He nuclei, in addition to alpha particles and energetic protons. Large fluxes of ^3He can readily interact with stable isotopes of intermediate mass nuclei and thereby produce short-lived radioactive species such as ^{26}Al , ^{36}Cl , and ^{41}Ca (Gounelle et al. 2001, 2006). Note that these species are also produced by supernovae (Woosley et al. 2002, Wadhwa et al. 2007). More importantly, however, these spallation reactions can produce the light isotopes ^7Be and ^{10}Be , species that are not produced via stellar nucleosynthesis, and hence are not explained by supernova enrichment. The detection of ^{10}Be in an Allende inclusion (McKeegan et al. 2000) thus argues for internal irradiation (Gounelle et al. 2001). However, this latter conclusion assumes that ^{10}Be cannot be produced via spallation from Galactic cosmic rays, and this claim has been disputed (Desch et al. 2004).

It is important to keep in mind that ^{60}Fe cannot be produced through internal irradiation and hence requires an external source. Current data from meteorites can thus be interpreted to suggest that both external and internal enrichment mechanisms are required. Specifically, the local enrichment scenario has difficulty producing ^{60}Fe , which argues for a supernova origin; in contrast, ^{10}Be is produced only by spallation processes, which argues for internal enrichment.

6.4. Distributed Supernova Enrichment

Although ^{60}Fe must be produced through stellar nucleosynthesis, the enrichment of the early solar nebula does not necessarily require a single supernova source. The generally accepted abundance of ^{60}Fe is quoted in Table I, but measurements of this quantity remain uncertain. For example, this value could actually be an upper limit, with the true abundance lower by a factor of ~ 3 (see Gounelle & Meibom 2008, and references therein). In light of

this possible revision, one recent model suggests that a collection of supernovae, all taking place within the same molecular cloud over at timescale of 10 – 20 Myr, could account for the observed iron abundances (Gounelle et al. 2009).

Since one supernova is a low probability event, one might worry that a collection of supernovae would be rare: Consider a $10^6 M_{\odot}$ molecular cloud. With typical star formation efficiencies, the cloud can produce perhaps 3×10^4 stars over the 10 – 20 Myr time span of interest. Given the IMF presented in Section 2.1, this population of stars is expected to produce ~ 140 supernova progenitors (with masses $m \geq 8$). However, this potential ~ 100 -fold increase in supernova numbers (compared with enrichment by a single event) must be balanced against the increased source distances and the loss of material through radioactive decay (the half-life of ^{60}Fe is only ~ 2 Myr). On the other hand, the target area for capture is greatly increased, and the fact that injection takes place in a diffuse phase helps efficiency. In addition, the point-to-point variation in the amount of ^{60}Fe produced could be substantial, so that Sun could form in a region with a positive fluctuation in ^{60}Fe abundance. Finally, we note that recent measurements (Rugel et al. 2009) suggest that the half-life for ^{60}Fe could be longer (about 2.5 Myr) than the accepted value (1.5 Myr), which would make this distributed enrichment scenario easier to realize.

Recent work (Connelly et al. 2008) measures the age of the lead system ^{207}Pb – ^{206}Pb in the chondrules of Allende, and finds an age of 4565.45 ± 0.45 Myr. This age is younger than the standard age for calcium-aluminum-rich inclusions (CAIs), and agrees with the ages found for the ^{26}Al – ^{26}Mg system. Further, these isotopes are inferred to be distributed homogeneously throughout the solar nebula (Villeneuve et al. 2009). Since the lead isotopes arise from stellar nucleosynthesis, this finding offers support for the theory of supernova enrichment of ^{26}Al . On the other hand, if these nuclear species were injected by a single supernova, the ^{26}Al might not have been so evenly distributed across the early solar nebula (whereas internal irradiation and/or distributed supernovae could account for this homogeneity).

6.5. Other Enrichment Scenarios

Although the current consensus holds that short-lived radioactive nuclei are provided to the early solar system by either supernovae or internal sources — or perhaps both — one should keep in mind that other possibilities exist. For example, thermally pulsating asymptotic giant branch (AGB) stars have been suggested as an enrichment source (Busso et al. 1999, 2003). Since these stars only provide radioactive nuclei at the end of their lives, and since their main-sequence lifetimes are long, the probability that such a source would be associated with a molecular cloud is relatively low (Kastner & Myers 1994). The abundance

yields work best for AGB stars of intermediate mass $M_* = 3 - 5 M_\odot$ (Wasserburg et al. 2006), and such stars have main-sequence lifetimes in the range 70 – 200 Myr. These timescales are thus longer than the lifetimes of molecular clouds, and hence the timing problem for seeding the early solar nebula is more severe for models using AGB stars than for models using supernovae. Nonetheless, enrichment scenarios using asymptotic giant branch stars have been constructed (Trigo-Rodriguez et al. 2008) and should be considered further.

Wolf-Rayet stars represent another external source of radioactive nuclei for the early solar nebula. This enrichment mechanism still requires a massive star, here with progenitor mass $M_* > 60 M_\odot$ (Arnould et al. 1997), but without the explosion. Since such massive stars are much rarer than those required for supernova enrichment, this scenario is somewhat less probable. In this case we make a quantitative estimate using equation (24): The chances of finding a 60 solar mass star are smaller than the chances of finding a 25 solar mass star by a factor of ~ 5.5 . On the other hand, the stellar lifetime is shorter (~ 5 Myr), which helps with timing issues. Notice also that Wolf-Rayet winds could supply some fraction of the observed short-lived radio isotopes, ^{26}Al for example (Gaidos et al. 2009), in addition to enrichment from other sources (supernovae and/or internal irradiation).

Finally, for completeness, we reiterate that short-lived radio isotopes not only provide constraints on the environment in which the Sun formed, but also provide heating sources (Hester & Desch 2005). For example, the decay of ^{26}Al provides a substantial supply of energy for the differentiation of planetesimals (Grimm & McSween 1993). On the other hand, the X-wind mechanism, which can provide internal nuclear enrichment, also acts as a heating source (Lee et al. 1998). Elaborate models have been constructed (Shang et al. 2000, Shu et al. 2001) to account for the signatures of heating found in both chondrules and CAIs.

7. SUMMARY

7.1. Overview of Results

This review has outlined a number of constraints on the star formation process that produced our Solar System. The first set of issues concerns the general properties of our Sun and planets, and provides us with an assessment of whether Sun-like systems are common or rare. The Sun is a relatively massive star (Section 2.1) and stars this large are expected to form 12 percent of the time. The Sun is a single star, which occurs about 30 percent of the time for solar-mass stars, but more often for the general stellar population (Section 2.2). The Sun has relatively high metallicity (Section 2.3), placing our solar system in the top 25

percent. Our Solar System has successfully made giant planets, a feat that is accomplished by about 20 percent of solar-type stars (Section 2.4). The outer edge of the solar system (Section 2.5) indicates that the early solar nebula extended out to 30 – 50 AU, a size that is typical among star/disk systems observed today. All of these required features of the Solar System are thus relatively common.

It is important to keep in mind that the chances of a solar system realizing all of the properties outlined above are far from guaranteed. For example, we can write down an analog of the Drake equation to assess the combined probability \mathcal{P}_\odot for a given solar system to have the above characteristics,

$$\mathcal{P}_\odot = \mathcal{F}_1 \mathcal{F}_Z \mathcal{F}_B \mathcal{F}_P \dots \leq 0.0018, \quad (31)$$

where the factors correspond to the probabilities for a solar system to have at least a one solar mass star, at least solar metallicity, no binary companion, form giant planets, and so on. The numerical value on the right hand side of the equation provides an upper limit to the probability, provided that the factors are statistically independent. Although this probably is low (less than one percent), one should not conclude that that solar systems like ours are rare or unusual. The necessity of having a large number of relatively common properties results in a low probability for the combination to occur. However, with ~ 100 billion stars in the Galaxy, the probability would have to be much lower for our Solar System to be considered unusual (see also the discussion of Gustafsson 2008).

The above considerations are (mostly) independent of the particular birth environment of the Sun. Additional properties of the Solar System allow us to constrain the properties of the solar birth cluster. We first consider dynamical constraints (Section 4): The observed planetary orbits indicate that no passing stars have made disruptive close encounters with the Solar System after the giant planets were produced, where the closest possible approach is about 225 AU. The early solar nebula extended out to approximately 30 AU, which indicates that no passing star came closer than about 100 AU at earlier epochs. On the other hand, the observed orbital elements of the dwarf planet Sedna can be understood if a close encounter did take place, where the required distance of closest approach $b = 400 - 800$ AU. Stellar encounters at much closer distances tend to produce too many Sedna-like objects, so that closer encounters are unlikely. All of these system properties can thus be understood if the early solar system experienced an encounter with a distance of closest approach $b \sim 400$ AU. This requirement, in turn, constrains the stellar density n_* of the birth environment and the Solar System’s residence time t in that region (Section 4.4) so that $\langle n_* t \rangle \approx 80,000 \text{ pc}^{-3} \text{ Myr}$. Since the typical mean stellar density is only of order $n_* \sim 100 \text{ pc}^{-3}$, the Solar System must live within its birth cluster a relatively long time (perhaps a few hundred million years), or live in a somewhat higher density environment, in order to experience the required close

encounter. Only relatively large bound clusters, those with $N \geq 1000$, are expected to live that long (Binney & Tremaine 1987, Kroupa et al. 2001, Lamers et al. 2005).

Clusters also provide external radiation fields that affect the forming Solar System, primarily by evaporating the early solar nebula (Section 5). Although cluster environments provide both EUV and FUV radiation, the latter tends to dominate the photoevaporation of disks (Figures 3 and 4). An external FUV flux with $G_0 = 3000$ will evaporate the outer part of the solar nebula (beyond about 36 AU) over 10 Myr, the typical timescale for disks to survive and for giant planets to form. Since the nebula must have retained its gas within Neptune’s orbit (Section 2), the FUV flux cannot be much larger than this benchmark value. Although the solar nebula could have formed with an outer radius $r_d \sim 30$ AU, the disk could also have been larger, and we can assess what type of cluster is necessary to provide an explanation for this outer radius through photoevaporation: The required radiation field is about $G_0 \approx 10^4$ (Figure 4), a value that is cleanly beyond the peak of the distribution for young clusters in the solar neighborhood (Figure 2). As a result, the birth cluster must be relatively large, say, with $N \geq 1000$. Note that the Solar System could have been born within an even larger cluster, provided that it (primarily) resided at large radii until the gas giant planets were produced.

The next set of constraints on the solar birth cluster arises from the required presence of short-lived radio isotopes (Section 6). As outlined above, some fraction of short-lived radioactive species must have an origin from stellar nucleosynthesis, so that some enrichment from a nearby supernova is indicated. The preferred starting mass for the exploding star is $M_* \sim 25M_\odot$. In addition to providing a good mix of short-lived radioactive isotopes, this mass scale is suggested by cluster considerations: Smaller stars spend too much time on the main-sequence and make the timing issues more problematic. Larger stars are exceedingly rare, which pushes the required cluster size to larger N (see equation [26]), which in turn leads to greater disruption of the solar nebula. Given the need for a large progenitor mass, and the rarity of massive stars, supernova enrichment requires a large solar birth cluster with $N \geq 1000$ (see Figure 5). In addition, at the time of the supernova explosion, the solar nebula must be close enough to capture a sufficient amount of ejecta (equation [27]) and yet far enough away to survive the blast (Figure 6). This compromise implies that the Solar System had to be roughly 0.2 pc from the explosion, which most likely occurred near the cluster center (Section 6.1). Keep in mind that these constraints can be alleviated if some of the observed nuclear enrichment arises from internal sources (Section 6.3) and/or distributed supernovae (Section 6.4).

These constraints are summarized in Table II, which lists the effects outlined above, their implications, and the fraction of forming solar systems that are expected to meet each

requirement. These fractions are approximate and are thus subject to future revision. The top four entries correspond to Solar System properties that are largely independent of the birth environment, whereas the bottom entries depend on the cluster properties. To assess the odds of a solar system being born within a cluster of membership size N , we assume that the probability is uniform-logarithmically distributed in N (Section 3.1), and then use either dynamical considerations (Section 4) or supernova probability distributions (Section 6.1 and Figure 5). To assess the odds of the Solar System residing at a given radial location, we use the dP/dr distributions discussed in Section 3.2 with density profile $n_* \propto r^{-2}$ (the form expected for more evolved clusters) and the cluster radius law $R \propto N^{1/3}$. Note that the probability of surviving the supernova ($d \geq 0.1$ pc) is not independent of the probability of receiving enough ejecta ($d \leq 0.3$ pc), so that the joint probability is not their product (see equation [30]). The odds of a solar system experiencing a given FUV radiation field is determined from the flux distribution shown in Figure 2. Notice that each individual constraint on the early solar system is likely to be satisfied with reasonably high probability. In this sense, our particular star and planetary system are not rare or unusual. However, as discussed above, the likelihood of a solar system meeting all of these conditions is much lower (less than 1 percent).

Table II: Summary of Constraints

Solar System Property	Implication	Fraction
Mass of Sun	$M_* \geq 1M_\odot$	0.12
Solar Metallicity	$Z \geq Z_\odot$	0.25
Single Star	(not binary)	0.30
Giant Planets	(successfully formed)	0.20
Ordered Planetary Orbits	$N \leq 10^4$	0.67
Supernova Enrichment	$N \geq 10^3$	0.50
Sedna-Producing Encounter	$10^3 \leq N \leq 10^4$	0.16
Sufficient Supernova Ejecta	$d \leq 0.3$ pc	0.14
Solar Nebula Survives Supernova	$d \geq 0.1$ pc	0.95
Supernova Ejecta and Survival	$0.1 \text{ pc} \leq d \leq 0.3 \text{ pc}$	0.09
FUV Radiation Affects Solar Nebula	$G_0 \geq 2000$	0.50
Solar Nebula Survives Radiation	$G_0 \leq 10^4$	0.80

7.2. Scenarios for the Solar Birth Aggregate

Although the birth environment of the Solar System is significantly constrained, one can find working scenarios that meet all of the observational requirements. As a starting point, this section explores the case where the Sun formed within a moderately large cluster with $N = 10^3 - 10^4$, and outlines the cluster properties and other considerations that are necessary to explain the observed system properties. This solution is not unique, and it contains significant shortcomings. Both of these issues are discussed below, as well as some alternatives. In spite of the uncertainties, this discussion demonstrates that a working scenario can be found, and illustrates the highly constrained nature of the problem.

Most stars form in clusters of some size N . External enrichment of short-lived radioisotopes suggests a cluster with at least $N \geq 1000$ in order to have a reasonable chance of producing a $25 M_{\odot}$ star (the preferred progenitor mass for nuclear enrichment). However, stellar models show that nucleosynthesis cannot provide the early solar nebula with the full inventory of short-lived radio isotopes (including ^{26}Al , ^{36}Cl , ^{41}Ca , and ^{60}Fe). For example, models with a $M_* = 25M_{\odot}$ progenitor can provide the correct abundances of ^{26}Al , ^{41}Ca , and ^{60}Fe , but fail to produce the abundance of ^{36}Cl by a factor of ~ 100 (Meyer 2005). This discrepancy thus argues for a dual origin of the radionuclides of intermediate atomic number (e.g., Gounelle et al. 2006). This point of view is bolstered by the discovery of the light isotopes ^7Be and ^{10}Be , which must be produced by spallation rather than nucleosynthesis in stars. In this scenario, local irradiation models produce the light isotopes, while a supernova produces the proper abundance of ^{60}Fe . Both stellar nucleosynthesis and local irradiation models can deliver ^{26}Al , ^{36}Cl , ^{41}Ca . For completeness, note that a faint supernova with mixing and fallback can also help explain the initial abundance patterns of the short-lived radio isotopes (Takigawa et al. 2008). In addition, distributed supernovae can produce ^{60}Fe (Gounelle & Meibom 2008), and the ^{60}Fe half-life could be longer (Rugel et al. 2009), which would alleviate the some of the constraints implied by the observed iron abundances.

Clusters in this membership size range $N = 10^3 - 10^4$ produce strong radiation fields and significant probabilities for close encounters. Although both of these effects can potentially cause disruption, the early Solar System stands a good chance of surviving unscathed. On the other hand, the requirement of an encounter with $b \sim 400$ AU to explain the observed orbit of Sedna also argues for a birth cluster in the approximate range $N = 10^3 - 10^4$. Close encounters are relatively rare in clusters with $N \leq 1000$, in part because of their short lifetimes; close encounters become more likely with increasing N , so that bound clusters with $N \geq 10^4$ are sufficiently long-lived that severe disruption becomes likely. Note that the need for a Sedna-producing encounter implies that the Sun formed within a gravitationally bound cluster, which occurs about 10 percent of the time. The radiation from a cluster in this size

range will provide some disk evaporation, but the early solar nebula can survive (for radii $r \leq 30$ AU) as long as the Solar System does not reside in the core of the cluster. However, when the supernova explosion ignites, the solar nebula must be only about 0.2 pc away, which places it relatively near the core, certainly in the inner portion of the cluster. These location restrictions lower the odds of the Solar System achieving successful enrichment (see equation [30]).

The timing requirements provide additional tight constraints on the supernova enrichment hypothesis: The Sun and the progenitor are most likely to form at nearly the same epoch, consistent with observations of narrow age spreads in embedded young clusters. The progenitor can burn through its fuel and then explode ~ 7.5 Myr later. At this time, the solar nebula could still have enough mass to capture the required ejecta (with the observed disk “half-life” of ~ 3 Myr, about 20 percent of disks live this long). Nonetheless, this picture works better if the Solar System forms somewhat later, with a time offset of a few to several Myr. For completeness we note that recent measurements (Bizzarro et al. 2007) suggest that the oldest planetesimals formed in the absence of ^{60}Fe , with a ~ 1 Myr time delay between the oldest bodies and those that contain ^{60}Fe ; however, although this data work in favor of the late enrichment picture, subsequent work indicates that iron meteorites have the same isotopic composition as the Earth, and hence does not find evidence for this time difference (Dauphas et al. 2008). Notice that if the progenitor has an even larger mass, its pre-explosion lifetime is shorter, but the probability of a given cluster producing such a large star decreases. Relatively soon after the explosion, giant planet formation is complete, but the Solar System remains in its birth cluster. After this time, at an age of about 10 Myr, radiation from the background cluster has a less destructive influence. The Solar System must stay inside the cluster long enough for a close encounter to provide Sedna with its observed orbital elements and perhaps to help truncate the outer edge of the Kuiper belt. After this close encounter, most likely when the cluster age is 10 – 100 Myr, the Solar System leaves its birth cluster with minimal additional disruption.

This picture of the solar birth aggregate is specified further by the probability distributions shown in Figure 7. The solid curve shows the probability of a cluster producing a $M_* = 25 M_\odot$ star as a function of stellar membership size N . The two dashed curves show the probability that the solar nebula experiences an encounter close enough to explain Sedna ($b \sim 400$ AU) and does not experience an encounter so close that the orbital elements of the planets are significantly changed ($b \sim 225$ AU). To produce these curves, we have used the cluster properties outlined in Section 3.2, including the lifetime estimate for bound clusters (from Lamers et al. 2005). The dotted curve shows the probability for the Solar System to experience an FUV radiation field less intense than $G_0 = 10^4$; larger values would evaporate too much gas from the region of the disk that produces giant planets. This condition requires

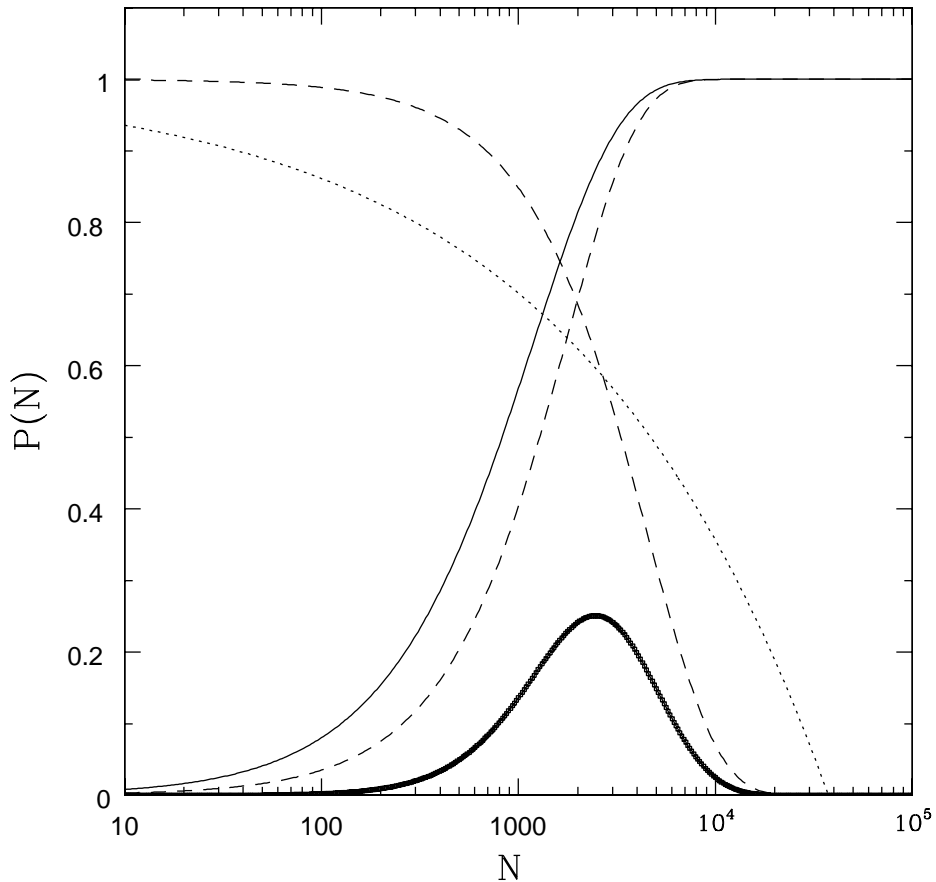


Fig. 7.— Probability of the solar birth cluster meeting several constraints as a function of stellar membership size N . Solid curve shows the probability of the cluster producing a supernova with progenitor mass $M_* \geq 25M_\odot$. The dashed curves show the probability of a close encounter with $b \leq 400$ AU (to produce Sedna), but no encounters with $b \leq 225$ AU (to preserve planetary orbits). Dotted curve shows the probability of the FUV radiation field having $G_0 \leq 10^4$. The heavy bell-shaped curve shows the joint probability distribution, for which $\langle N \rangle = 4300 \pm 2800$. These constraints are necessary but not sufficient: For successful nuclear enrichment, the Solar System must also be located the proper distance from the supernova and satisfy the corresponding timing constraints (see text).

the Solar System to reside in the outer part of the cluster, where we have used the radial probability distribution of equation (9). If the constraints are independent, the probability of the Solar System realizing all of these conditions is given by their product, which is shown by the dark bell-shaped curve. This joint probability distribution has an expectation value and variance such that $\langle N \rangle \approx 4300 \pm 2800$, consistent with the previously quoted range $N = 10^3 - 10^4$.

The distributions shown in Figure 7 only place limits on the membership size N of the putative birth cluster. Additional requirements are necessary for successful supernova enrichment, e.g., the timing of the supernova and the Solar System location within the cluster. As a result, the constraints represented by Figure 7 are necessary but not sufficient. Note that the constraints from supernova enrichment can be mitigated, or perhaps eliminated, if the short-lived radio isotopes are produced by internal irradiation and distributed supernovae. However, the requirement of a close encounter to explain Sedna implies almost the same constraint on the cluster size N as the requirement of a $25 M_{\odot}$ progenitor (see Figure 7). As a result, the need for a cluster with $N = 10^3 - 10^4$ remains.

A wide range of previous studies — often using different properties of the Solar System to provide constraints — have considered the birth environment of the Sun. In spite of this diversity, many of these estimates are roughly consistent with the description given above: A number of authors have highlighted the need for the Sun to form within some type of cluster in order for supernova enrichment to take place (Cameron & Truran 1977, Vanhala & Boss 2002, Tachibana et al. 2006, Looney et al. 2006, Megeath et al. 2008). The need for both supernova enrichment and limited planetary scattering implies a solar birth cluster with $N \approx 2000 \pm 1000$ (Adams & Laughlin 2001). On the other hand, a close encounter with another star in the birth cluster may be required to explain the observed orbital elements of Sedna, and perhaps the Kuiper Belt (Brasser et al. 2006, Kenyon & Bromley 2004, Morbidelli & Levison 2004), which suggests that $N \approx 10^3 - 10^4$ (see also Malmberg et al. 2007). A similar study suggests that $N = 500 - 3000$, with cluster radius $R = 1 - 3$ pc (Portegies Zwart 2009). If planet scattering is not considered, the expected value of cluster membership size N increases. If a large dense cluster is invoked, so that a large fraction of stars reside near the center, the cluster membership estimate increases to $N \approx 3 \times 10^5$, with an expected supernova progenitor mass $M_* = 75 M_{\odot}$ (Williams & Gaidos 2007). Even more interactive environments, analogous to the star forming region in the Eagle Nebula, have also been suggested (Hester et al. 2004). The radiation fields provided by young clusters are potentially disruptive (Armitage 2000), but the early solar nebula can survive in clusters with $N \leq 10^4$ if it spends enough time in the outer regions (Scally & Clarke 2001, Mann & Williams 2009). Finally, chemical considerations suggest that the Sun formed in the presence of strong FUV radiation fields, where rough estimates

indicate a birth cluster with $N \sim 4000$ (Lee et al. 2008). Although uncertainties remain, these studies thus suggest that the membership size of the solar birth cluster should fall in the range $N \approx 10^3 - 10^4$.

7.3. Implications for Star and Planet Formation

This review of the possible birth environments for the Sun provides an important consistency check on our current paradigms of star formation and planet formation. The above considerations suggest that our Solar System is likely to have formed within a moderately large cluster with $N = 10^3 - 10^4$, and that the early solar nebula could have been enriched through both an external supernova and internal irradiation. The necessary cluster systems are relatively common, with the Trapezium Cluster in Orion being the closest analog. On a related note, each of the individual properties of our Solar System that are affected by the birth environment can be realized with reasonably high probability (Table II). We thus conclude that the required formation environment of the Sun is neither rare nor unusual. On the other hand, the odds of a solar system realizing a particular combination of a large number of requirements is relatively low. A quantitative assessment of the *a priori* odds of realizing all of these properties of our Solar System is difficult to determine, and should be the subject of further work.

Turning the problem around, this discussion of the solar birth environment informs our understanding of star and planet formation: We find that the effects of the birth cluster are neither negligible nor dominant. The cluster environment can readily sculpt the early solar nebula, and hence other circumstellar disks, through truncation by passing stars and especially through evaporation. The resulting planetary systems can be shaped further by their environment, for example by changing orbital elements, primarily for companions with large semimajor axis. Circumstellar disks can acquire significant quantities of radioactive isotopes from nearby massive stars, and these nuclei affect their thermal structure. Solar systems can also gain mass from their environment and readily exchange rocky material with each other. The clusters provide ionizing photons, which affect magnetic coupling of both protostellar cores and circumstellar disks. On the other hand, major catastrophic events are rare: Disks are generally not compromised so much that giant planet formation can no longer (in principle) take place. Planetary ejection events, driven by outside influences, are also rare. On average, the cluster environment thus exerts an intermediate level of influence in determining solar system properties. Of course, solar systems living with cluster cores are affected to a much greater extent than those in the periphery. On a related note, the effects of clusters on forming solar systems must be assessed in statistical terms. One important

challenge for the future is thus to determine more accurate probability distributions for each of the effects discussed herein. We can then understand in greater detail how the background environment affects the formation of our Solar System, and others.

Acknowledgments

This review benefited from discussions with a large number of colleagues. I would especially like to thank E. Bergin, M. Duncan, M. Gounelle, H. Levison, A. Morbidelli, and J. Williams for their valuable input regarding the manuscript. This work was supported at the University of Michigan through the Michigan Center for Theoretical Physics. Portions of this work were carried out at the Isaac Newton Institute for Mathematical Sciences at Cambridge University. FCA is supported by NASA through the Origins of Solar Systems Program (grant NNX07AP17G), by NSF through the Division of Applied Mathematics (grant DMS-0806756), and by the Foundational Questions Institute (grant RFP1-06-1).

REFERENCES

- Abt H. 1983. *Annu. Rev. Astron. Astrophys.* 21:343
- Adams FC, Hollenbach D, Gorti U, Laughlin G. 2004. *Ap.J.* 611:360
- Adams FC, Laughlin G. 2001. *Icarus* 150:151
- Adams FC, Myers PC. 2001. *Ap.J.* 553:744
- Adams FC, Proszkow EM, Fatuzzo M, Myers PC. 2006. *Ap.J.* 641:504
- Adams FC, Spergel DN. 2005. *Astrobiology* 5:497
- Allen RL, Bernstein GM, Malhotra R. 2000. *Ap.J.* 542:964
- Allen L. et al. 2007. in *Protostars and Planets V.* ed. B Reipurth, D Jewitt, K Keil, pp. 361–376, Tucson: Univ. Arizona Press
- Allison RJ, Goodwin SP, Parker RJ, de Grijs R, Portegies Zwart SF, Kouwenhoven MBN. 2009. *Ap.J.* 700:99
- Andrews SM, Wilner DJ, Hughes AM, Qi C, Dullemond CP. 2009. *Ap.J.* 700:1502
- Armitage PJ. 2000. *Astron. Astrophys.* 362:968
- Arnould M, Paulus G, Meynet G. 1997. *Astron. Astrophys.* 321:452
- Balbus S, Hawley J. 1991. *Ap.J.* 376:214
- Battinelli P, Capuzzo-Dolcetta R. 1991. *MNRAS* 249:76
- Belbruno E, Moro-Martin A, Malhotra R. 2008. submitted to *Astron. J.* arXiv:0808.3268
- Bernstein GM. et al. 2004. *Astron. J.* 128:1364
- Binney J, Tremaine S. 1987. *Galactic Dynamics*, Princeton: Princeton Univ. Press
- Bizzarro M, Ulfbeck D, Trinquier A, Thrane K, Connelly JN, Meyer BS. 2007. *Science* 316:1178
- Bonnell IA, Davies MB. 1998. *MNRAS* 295:691
- Bonnell IA, Smith KW, Davies MB, Horne K. 2001. *MNRAS* 322:859
- Boss AP, Foster PN. 1998. *Ap.J.* 494:L103

- Brasser R, Duncan MJ, Levison HF. 2006. *Icarus* 184:59
- Brown ME, Trujillo C, Rabinowitz D. 2004. *Ap.J.* 617:645
- Busso M, Gallino R, Wasserburg GJ. 1999. *Annu. Rev. Astron. Astrophys.* 37:239
- Busso M, Gallino R, Wasserburg GJ. 2003. *Pub. Astron. Soc. Australia* 20:356
- Cameron AGW. 1993. in *Protostars and Planets III*. ed. EH Levy, JI Lunine, pp. 47–73, Tucson: Univ. Arizona Press
- Cameron, AGW, Hoefflich P, Myers PC, Clayton DD. 1995. *Ap.J.* 447:L53
- Cameron AGW, Truran JW. 1977. *Icarus* 30:447
- Carpenter JM. 2000. *Astron. J.* 120:3139
- Chandar R, Bianchi L, Ford HC. 1999. *Ap.J. Suppl.* 122:431
- Chevalier RA. 2000. *Ap.J.* 538:L151
- Clarke CJ. 2007. *MNRAS* 376:1350
- Clarke CJ, Pringle JE. 1993. *MNRAS* 261:190
- Connelly JN, Amelin Y, Krot AN, Bizzarro M. 2008. *Ap.J.* 675:L121
- Crida A. 2009. *Ap.J.* 698:606
- Cummings A, Butler PR, Marcy GW, Vogt SS, Wright JT, Fischer DA. 2008. *Pub. Astron. Soc. Pac.* 120:531
- Dauphas N, Cook DL, Sacarabany A, Fröhlich C, Davis AM, Wadhwa M, Pourmand A, Rauscher T, Gallino R. 2008. *Ap.J.* 686:560
- Desch SJ. 2007. *Ap.J.* 671:878
- Desch SJ, Connolly HC, Srinivasan G. 2004. *Ap.J.* 602:528
- Duncan M, Quinn T, Tremaine S. 1987. *Astron. J.* 94:1330
- Duquennoy A, Mayor M. 1991. *Astron. Astrophys.* 248:485
- Elmegreen BG, Efremov YN. 1997. *Ap.J.* 480:235
- Elmegreen BG, Clemens C. 1985. *Ap.J.* 294:523

- Ercolano B, Clarke CJ, Drake JJ. 2009. *Ap.J.* 699:1639
- Fatuzzo M, Adams FC. 2008. *Ap.J.* 675:1361
- Fatuzzo M, Adams FC, Melia F. 2006. *Ap.J.* 653:L49
- Gaidos EJ. 1995. *Icarus* 114:258
- Gaidos EJ, Krot AN, Williams JP, Raymond SN. 2009. *Ap.J.* 696:1854
- Gammie CF. 1996. *Ap.J.* 457:355
- Gladman B, Holman M, Grav T, Kavelaars J, Nicholson P, Aksnes K, Petit JM. 2002. *Icarus* 157:269
- Gorti U, Hollenbach D. 2009. *Ap.J.* 690:1539
- Goswami JN, Vanhala HAT. 2000. in *Protostars and Planets IV*. ed. V Mannings, AP Boss, SS Russell, pp. 963–994, Tucson: Univ. Arizona Press
- Gounelle M, Meibom A. 2008. *Ap.J.* 680:781
- Gounelle M, Meibom A, Hennebelle P, Inutsuka S. 2009. *Ap.J.* 694:L1
- Gounelle M, Shu FH, Shang S, Glassgold AE, Rehm KE, Lee T. 2001. *Ap.J.* 548:1051
- Gounelle M, Shu FH, Shang S, Glassgold AE, Rehm KE, Lee T. 2006. *Ap.J.* 640:1163
- Grimm R, McSween HY. 1993. *Science* 259:653
- Gustafsson B. 2008. *Physica Scripta* 130:014036
- Gutermuth RA, Megeath ST, Pipher JL, Williams JP, Allen LE, Myers PC, Raines SN. 2005. *Ap.J.* 632:397
- Gutermuth RA, Megeath ST, Myers PC, Allen LE, Pipher JL, Fazio GG. 2009. *Ap.J. Suppl.* 184:18
- Habing HJ. 1968. *B.A.I. Netherlands* 19:421
- Hartmann L. 2007. *Physica Scripta* 130:014012
- Hartmann L, Ballesteros-Paredes J, Bergin EA. 2001. *Ap.J.* 562:852
- Hayashi C. 1981. *Prog. Theor. Phys. Suppl.* 70:35

- Heggie DC, Rasio FA. 1996. *MNRAS* 282:1064
- Heller CH. 1995. *Ap.J.* 455:252
- Henry TJ, Kirkpatrick JD, Simons DA. 1994. *Astron. J.* 108:1437
- Hernández J et al. 2007. *Ap.J.* 662:1067
- Hester JJ, Desch SJ. 2005. in *Chondrites and the Protoplanetary Disk*. ASP Conference Series, Vol. 341. ed. AN Krot, ERD Scott, B Reipurth, pp. 107–130, San Francisco: Astron. Soc. Pacific
- Hester JJ, Desch SJ, Healy KR, Leshin LA. 2004. *Science* 304:1116
- Hillenbrand LA. 1997. *Astron. J.* 113:1733
- Hollenbach D, Johnstone D, Lizano S, Shu FH. 1994. *Ap.J.* 428:654
- Isella A, Carpenter JM, Sargent AI. 2009. *Ap.J.* 701:260
- Jijina J, Myers PC, Adams FC. 1999. *Ap.J. Suppl.* 125:161
- Johnstone D, Hollenbach D, Bally J. 1998. *Ap.J.* 499:758
- Kaib AN, Quinn T. 2008. *Icarus* 197:221
- Kastner JH, Myers PC. 1994. *Ap.J.* 421:605
- Kaufman M, Wolre M, Hollenbach D, Luhman M. 1999. *Ap.J.* 527:795
- Kenyon SJ, Bromley BC. 2001. *Astron. J.* 121:538
- Kenyon SJ, Bromley BC. 2004. *Nature* 432:598
- Kobayashi H, Ida S. 2001. *Icarus* 153:416
- Krot AN, Amelin Y, Cassen P, Meibom A. 2005a. *Nature* 436:989
- Krot AN, Yurimoto H, Hutcheon ID, MacPherson GJ. 2005b. *Nature* 434:998
- Krot AN, Nagashima K, Bizzarro M, Huss GR, Davis AM, Meyer BS, Ulyanov AA. 2008. *Ap.J.* 672:713
- Kroupa P. 1995. *MNRAS* 277:1507
- Kroupa P, Aarseth S, Hurley J. 2001. *MNRAS* 321:699

- Kroupa P, Boily CM. 2002. *MNRAS* 336:1188
- Lada CJ, Lada EA. 2003. *Annu. Rev. Astron. Astrophys.* 41:57
- Lada CJ. 2006. *Ap.J.* 640:63
- Lamers HJGLM, Gieles M, Portegies Zwart SF. 2005. *Astron. Astrophys.* 429:173
- Larson RB. 1985. *MNRAS* 214:379
- Lee JE, Bergin EA, Lyons JR. 2008. *Meteor. Plan. Sci.* 43:1351
- Lee T, Shu FH, Shang H, Glassgold AE, Rehm KE. 1998. *Ap.J.* 506:898
- Levison HF, Morbidelli A, Dones L. 2004. *Astron. J.* 128:2553
- Lissauer JJ, Stevenson DJ. 2007. in *Protostars and Planets V.* ed. B Reipurth, D Jewitt, K Keil, pp. 591–606, Tucson: Univ. Arizona Press
- Looney LW, Tobin JJ, Fields BF. 2006. *Ap.J.* 652:1755
- Luu JX, Jewitt DC. 2002. *Annu. Rev. Astron. Astrophys.* 40:63
- Lyons JR, Young ED. 2005. *Nature* 435:317
- Maschberger Th, Clarke CJ. 2008. *MNRAS* 391:711
- Malmberg D, Davies MB. 2009. *MNRAS* 394:L26
- Malmberg D, de Angeli F, Davies MB, Church RP, Mackey D, Wilkinson MI. 2007. *MNRAS* 378:1207
- Mann RK, Williams JP. 2009. *Ap.J.* 694:L36
- McKee CF, Ostriker EC. 2007. *Annu. Rev. Astron. Astrophys.* 25: 565
- McKeegan KD, Chaussidon M, Robert F. 2000. *Science* 289:1334
- Megeath ST, Gaidos E, Hester JJ, Adams FC, Bally J, Lee JE, Wolk S. 2008. in *14th Cambridge Workshop on Cool Stars Stellar Systems and the Sun.* ASP Conference Series Vol. 384. ed. G van Belle, pp. 393–401, San Francisco: Astron. Soc. Pacific
- Meyer BS. 2005. in *Chondrites and the Protoplanetary Disk.* ASP Conference Series, Vol. 341. ed. AN Krot, ERD Scott, B Reipurth, pp. 515–526, San Francisco: Astron. Soc. Pacific

- Moeckel N, Bonnell IA. 2009. submitted to *MNRAS*, arXiv:0908.0253
- Montmerle T, Augereau J-C, Chaussidon M, Gounelle M, Marty B, Morbidelli A. 2006. *Earth, Moon, and Planets* 98:39
- Morbidelli A, Levison HF. 2004. *Astron. J.* 128:2564
- Ostriker EC. 1994. *Ap.J.* 424:292
- Ouellette N, Desch SJ, Hester JJ. 2007. *Ap.J.* 662:1268
- Peretto N, André P, Belloche A. 2006. *Astron. Astrophys.* 445:979
- Pfalzner S. 2009. *Astron. Astrophys.* 498:37
- Porras A, Christopher M, Allen LE, Di Francesco J, Megeath ST, Myers PC. 2003. *Astron. J.* 126:1916
- Portegies Zwart SF. 2009. *Ap.J.* 696:L13
- Preibisch T, et al. 2005. *Ap.J. Suppl.* 160:401
- Proszkow EM. 2009. *PhD Thesis* University of Michigan
- Proszkow EM, Adams FC. 2009. *Ap.J. Suppl.* 185:486
- Proszkow EM, Adams FC, Hartmann LW, Tobin JJ. 2009. *Ap.J.* 697:1020
- Rauscher T, Heger A, Hoffman RD, Woosley SE. 2002. *Ap.J.* 576:323
- Rocha-Pinto HJ, Maciel WJ. 1996. *MNRAS* 279:447
- Rugel G, Faestermann T, Knie K, Korschinek G, Poutivtsev M, Schumann D, Kivel N, Günther-Leopold I, Weinreich R, Wohlmuther M. 2009. *Phys. Rev. Lett.* 103:2502
- Salpeter EE. 1955. *Ap.J.* 121:161
- Scally A, Clarke C. 2001. *MNRAS* 325:449
- Scalo JM. 1998. in *The Stellar Initial Mass Function*. ASP Conf. Series Vol. 142. ed. G Gilmore, D. Howell, pp. 201–236, San Francisco: Astron. Soc. Pacific
- Schneider J. 2009. *Extrasolar Planets Encyclopedia* <http://exoplanet.eu/catalog-all.php>
- Shang S, Shu FH, Lee T, Glassgold AE. 2000. *Space Sci. Rev.* 92:153

- Shu FH. 1992. *Gas Dynamics: The Physics of Astrophysics*, Mill Valley: Univ. Science Books
- Shu FH, Adams FC, Lizano S. 1987. *Annu. Rev. Astron. Astrophys.* 25:23
- Shu FH, Johnstone D, Hollenbach D. 1993. *Icarus* 106:92
- Shu FH, Najita J, Ostriker E, Wilkin F, Ruden S, Lizano S. 2004. *Ap.J.* 429:781
- Shu FH, Shang S, Gounelle M, Glassgold AE, Lee T. 2001. *Ap.J.* 548:1029
- Smith RL, Pontoppidan KM, Young ED, Morris MR, van Dishoeck EF. 2009. *Ap.J.* 701:163
- Snider KD, Hester JJ, Desch SJ, Healy KR, Bally J. 2009. *Ap.J.* 700:506
- Spurzem R, Giersz M, Heggie DC, Lin DNC. 2009. *Ap.J.* 697:458
- Sterzik MF, Durisen RH. 1998. *Astron. Astrophys.* 339:95
- Störzer H, Hollenbach D. 1999. *Ap.J.* 515:669
- Tachibana S, Huss GR, Kita NT, Shimoda G, Morishita Y. 2006. *Ap.J.* 639:L87
- Takigawa A, Miki J, Tachibana S, Huss GR, Tominaga N, Umeda H, Nomoto K. 2008. *Ap.J.* 688:1382
- Testi L, Sargent AI, Olmi L, Onello JS. 2000. *Ap.J.* 540:L53
- Throop HB, Bally J. 2008. *Astron. J.* 135:2380
- Tobin JJ, Hartmann L, Furesz G, Mateo M, Megeath ST. 2009. *Ap.J.* 697:1103
- Trigo-Rodriguez JM, Garcia-Hernandez DA, Lugaro M, Karakas AI, van Raai M, Lario PG, Manchado A. 2008, arXiv:0812.4358
- Tsganis K, Gomes R, Morbidelli A, Levison FH. 2005. *Nature* 435:459
- Udry S, Santos NC. 2007. *Annu. Rev. Astron. Astrophys.* 45:397
- Umebayashi T, Nakano T. 2009. *Ap.J.* 690:69
- van den Bergh S. 1981. *Pub. Astron. Soc. Pac.* 93:712
- Vanhala HAT, Boss AP. 2002. *Ap.J.* 575:1144
- Villeneuve J, Chaussidon M, Libourel G. 2009. *Science* 325:985

- Wadhwa M, Amelin Y, Davis AM, Lugmair GW, Meyer B, Gounelle M, Desch SJ. 2007. in *Protostars and Planets V*. ed. B Reipurth, D Jewitt, K Keil, pp. 835–848, Tucson: Univ. Arizona Press
- Walsh AJ, Myers PC, Burton MG. 2004. *Ap.J.* 614:194
- Wasserburg GJ. 1985. in *Protostars and Planets II*. ed. DC Black, MS Matthews, pp. 703–737, Tucson: Univ. Arizona Press
- Wasserburg GJ, Busso M, Gallino R, Nollett KM. 2006. *Nuclear Phys. A.* 777:5
- Weidenschilling SJ. 1977. *Astrophys. Space Sci.* 51:153
- Wielen R, Fuchs B, Dettbarn C. 1996. *Astron. Astrophys.* 314:438
- Wielen R, Wilson TL. 1997. *Astron. Astrophys.* 326:139
- Williams JP, Gaidos E. 2007. *Ap.J.* 663:L33
- Wolszczan A. 1994. *Science* 264:538
- Woosley SE, Heger A, Weaver TA. 2002. *Rev. Mod. Phys.* 74:1015
- Young ED, Gounelle M, Smith RL, Morris MR, Pontoppidan KM. 2009. *Lunar Planetary Sci. Conf.* 40:1967